

# **Fabrication and Characterization of Knitted Silk-Based Composite Scaffold for Bone-Ligament-Bone (B-L-B) Graft**

A THESIS SUBMITTED FOR PARTIAL FULFILLMENT OF THE REQUIREMENT FOR  
THE DEGREE OF

**MASTER OF TECHNOLOGY**

**IN**

**BIOTECHNOLOGY**

**By**

**NIRAJ BABU**

**(Roll no. 212BM2008)**



Under the guidance of:

**Dr. BIBHUKALYAN PRASAD NAYAK**

**Department of Biotechnology and Medical Engineering**

**National Institute Of Technology Rourkela**

**2013-14**

## National Institute of Technology, Rourkela



### *Certificate*

This is to certify that the report entitled, “**Fabrication and Characterization of Knitted Silk-Based Composite Scaffold for Bone-Ligament-Bone (B-L-B) Graft**”, submitted by **Mr. NIRAJ BABU**, Roll No.: **212BM2008**, M.Tech-4th semester, Department of Biotechnology & Medical Engineering, National Institute of Technology, Rourkela (Deemed University) is an authentic work carried out by her under my supervision and guidance.

To the best of my knowledge, the matter embodied in the report has not been submitted to any other University / Institute for the award of any Degree or Diploma.

Date:

**Dr. B. P. NAYAK**

Department of Biotechnology & Medical Engineering

National Institute of Technology

Rourkela – 769008

## ACKNOWLEDGEMENT

It is said that curiosity is the mother of all inventions. If so, then I must be her favourite child. I dedicate this study to the tens and thousands of curiosity stricken science enthusiasts all over the world who work day in and out with a vision to understand the complexity of life and the living, to make the world a better place.

I would firstly like to thank my supervisor **Dr. Bibhukalyan Prasad Nayak** for endowing me with the current project and inculcating his faith in me that I can take it forward from my forerunners. Dr. Nayak is one of the few human beings whose passion for experimentation and ardent knowledge regarding the science has sparked the flame of curiosity in me. His keenness towards good and calmness in turmoil commands respect like no other.

I would also like to thank **Mr. Patitapabana Parida** for being so wonderfully enthusiastic about any venture that comes his way that he would put his heart and soul and those little tricks with tinkering fingers to help me out with the intricacies of my project.

A special mention to **Dr. Indranil Banerjee** and **Dr. Mukesh Gupta** for their timely advices and suggestions on how things are done right; and also for their ardent intellectual personality which translates as an inspiration towards persuasion in young minds like that of mine.

I am deeply indebted to each and every classmate of mine for making my two years of postgraduation however they turned out to be. Good or bad, I will take it as a big etch in the cornerstone of my soul to remember the lessons I have learned about people, society, culture and ways and rules of life. Special thanks to **Ms. Shumaila Khalid** for being by my side through my ups and downs and putting up with any illogical complications I had to endure during the tenure of this project.

I also thank NIT Rourkela for the wonderful infrastructure and beautiful architecture that provides a little bloom and life for this tiny city. For the few provisions that it could provide me with, I did try to make the best use of them during my stay here.

Lastly, but nowhere close to least, I send out a big bouquet of gratitude to my parents, **Mr. C. P. Babu** and **Mrs. Ambika Babu** for being such wonderful parents. No one would have been luckier than me to be in their shade and experience the freedom they have entrusted me with to explore any path in life as long as I am happy with it, regardless of any social obligations that I would have to compromise myself with. Thank you very much Dad for being such a big inspiration for me.

**Date:** 28.05.2014

**NIRAJ BABU**

## TABLE OF CONTENTS

(i)	ABSTRACT.....	(i)
(ii)	LIST OF FIGURES.....	(ii)
<b>1.</b>	<b>INTRODUCTION.....</b>	<b>1-7</b>
	1.1 Introduction	
	1.2 Anatomy and Physiology of the ACL	
	1.3 Enthesis	
	1.4 Tissue Engineering for ACL Regeneration	
	1.5 Objectives of the Study	
<b>2.</b>	<b>LITERATURE REVIEW.....</b>	<b>8-13</b>
<b>3.</b>	<b>PLAN OF WORK.....</b>	<b>14-15</b>
<b>4.</b>	<b>MATERIALS AND METHODS.....</b>	<b>16-27</b>
	4.1 Fabrication of Scaffold	
	4.1.1 Preparation of Silk Yarn	
	4.1.2 Knitting of Silk Scaffold	
	4.1.3 Morphological Characterization of Knitted Silk	
	4.1.4 Preparation of Phosphate Buffered Saline	
	4.1.5 Mechanical Strength Testing	
	4.2 Polymer Coating on Knitted Silk Scaffold	
	4.2.1 Preparation of Silk Solution	
	4.2.2 Alternate Soaking Process – Hydroxyapatite	

- 4.2.3 Freeze Drying Process – Silk/Chitosan Blend
- 4.2.4 Plain Coating – Polyvinyl Alcohol
- 4.3 Characterization Studies
  - 4.3.1 Water Absorption Studies
  - 4.3.2 Field Emission Scanning Electron Microscopy (FE-SEM)
  - 4.3.3 Fourier Transform Infrared Spectroscopy (FTIR)
  - 4.3.4 X-Ray Diffraction
- 4.4 Biocompatibility Studies
  - 4.4.1 Cell Culture
  - 4.4.2 Scaffold Sterilization
  - 4.4.3 Cell Adhesion Study
  - 4.4.4 Cell Seeding
  - 4.4.5 Cell Proliferation Study
- 4.5 Fabrication of Hybrid Scaffold

## **5. RESULTS AND DISCUSSIONS.....28-50**

- 5.1 Morphology of Scaffold
  - 5.1.1 Morphology of Knitted Scaffold
  - 5.1.2 Morphology of Hydroxyapatite Coating
    - 5.1.2.1 SEM Analysis of Hydroxyapatite Coating
    - 5.1.2.2 XRD Analysis of Hydroxyapatite Coating
    - 5.1.2.3 FTIR Analysis of Hydroxyapatite Coating
  - 5.1.3 Morphology of Silk/Chitosan Sponge
    - 5.1.3.1 XRD Analysis of Silk/Chitosan Sponge
  - 5.1.4 Morphology of Polyvinyl Alcohol

5.1.4.1 XRD of Polyvinyl Alcohol Coating	
5.2 Mechanical Strength Testing	
5.3 Water Absorption Studies	
5.3.1 Water Absorption Study for Hydroxyapatite	
5.3.2 Water Absorption Study for Silk/Chitosan	
5.3.3 Water Absorption Study for Polyvinyl Alcohol	
5.4 Biocompatibility Studies	
5.4.1 Cell Adhesion Study	
5.4.2 Cell Proliferation Study	
5.5 Properties of Hybrid Scaffold	
<b>6. CONCLUSION.....</b>	<b>51-52</b>
<b>7. REFERENCES.....</b>	<b>53-56</b>

## ABSTRACT

The Anterior Cruciate Ligament (ACL) is one of the four major ligaments of the knee. Protruding out from the notch of the femur it leads back into the femoral chondyle and then fixes deep within the tibia of the lower limb. Owing to its central position and key role in load bearing and flexing of the knee, it is known to be one of the most widely injured ligaments of the body. Scientists have been trying to engineer artificial ligaments by using novel scaffolds as a replacement of injured ligaments beyond repair, but have failed in the post-operative recovery stages due to the inability of the ligament-alone graft to satisfactorily integrate with the bone and provide adequate insertional strength. This was found to be due the lack of formation of a specialized fibrocartilaginous tissue known as the ‘enthesis’ at the junction between the bone and the ligament. The current project has focused on the fabrication of a silk-based knitted scaffold which comprises of three compartments, one each for the bone, ligament and enthesis tissues. With a motive to differentiate the MSCs into fibrocartilage lineages in enthesis compartment amidst the mature cell lines, an array of methods were adopted for surface modification of the compartmentalized knitted silk scaffold by using bio-polymers such as silk solution, chitosan, polyvinyl alcohol and hydroxyapatite on the appropriate compartments. The ligament and bone compartments were reserved for mature cell line culture. The various methods used for coatings of polymers over the knitted-silk were alternate soaking, plain coating and freeze-drying. The scaffold was characterized for various parameters such as water absorption, biodegradability, tensile strength, purity of coatings, and biocompatibility. It was concluded that the multi-compartment silk based scaffold developed in house has the novelty for tissue engineering the bridge component between bone and ligament i.e. fibrocartilaginous enthesis. Such a complex graft with incorporation of enthesis in laboratory can provide natural insertional strength at the interface and can change the current scenario of replacing injured ligaments.

**KEYWORDS:** *Enthesis, Anterior Cruciate Ligament, Tissue Engineering, Knitted Silk, Hydroxyapatite, Chitosan, Polyvinyl Alcohol*

## LIST OF FIGURES

**Figure 1:** Position of the ACL in the human knee

**Figure 2:** Knitted Silk scaffold fixed on (i) glass slide (ii) wire frame

**Figure 3:** Experimental setup of Alternate Soaking process for Hydroxyapatite coating on knitted silk based scaffold

**Figure 4:** Silk/Chitosan Blended solution for sponge overlaying on knitted silk based scaffold (i) before freezing (ii) after freezing

**Figure 5:** Cells used in the experiment (i) MG-63 and (ii) Saos-2

**Figure 6:** Morphological visualization of knitted silk based scaffold under SEM

**Figure 7:** Knitted silk scaffold after alternate soaking of hydroxyapatite (10 cycles)

**Figure 8:** SEM micrograph of hydroxyapatite coated knitted silk based scaffold after 5 cycles of alternate soaking process

**Figure 9:** SEM micrograph of hydroxyapatite coated knitted silk based scaffold after 10 cycles of alternate soaking process

**Figure 10:** SEM micrograph of hydroxyapatite coated knitted silk based scaffold after 15 cycles of alternate soaking process

**Figure 11:** SEM micrograph of hydroxyapatite coated knitted silk based scaffold after 20 cycles of alternate soaking process

**Figure 12:** XRD of alternate soaking experiment showing representative peaks of HA crystals on knitted silk based scaffold

**Figure 13:** FTIR analysis of alternate soaking process showing representative peaks of HA on knitted silk based scaffold

**Figure 14:** Silk/Chitosan sponges overlaid on knitted silk based scaffold (i) 2% (ii) 4% (iii) 6% and (iv) 8% silk/chitosan concentration

**Figure 15:** XRD of Silk/Chitosan sponge overlaid on knitted silk based scaffold

**Figure 16:** PVA coated knitted silk based scaffold (i) 4% (ii) 6% (iii) 8% (iv) 12%

**Figure 17:** XRD analysis of PVA coated knitted silk based scaffold



**Figure 18:** Mechanical strength testing of knitted silk based scaffold immersed in PBS over a period of time to analyze the degradation of the scaffold

**Figure 19:** Water absorption study of Hydroxyapatite coated knitted silk scaffold

**Figure 20:** Percentage of water absorption by hydroxyapatite scaffold

**Figure 21:** Water absorption study of silk/chitosan overlaid knitted silk based scaffold

**Figure 22:** Percentage of water absorption by silk/chitosan overlaid knitted silk based scaffold

**Figure 23:** Water absorption study of PVA coated knitted silk based scaffold

**Figure 24:** Percentage of water absorption by PVA coated knitted silk based scaffold

**Figure 25:** MTT assay to study proliferation of MG-63 on HA coated knitted silk based scaffold

**Figure 26:** MTT assay to study proliferation of Saos-2 on silk/chitosan and PVA coated knitted silk based scaffold

**Figure 27:** Water absorption study of hybrid knitted silk based scaffold

**Figure 28:** MTT assay to study the proliferation of Saos-2 on hybrid knitted silk scaffold

# **CHAPTER – 1**

## **INTRODUCTION**

## **1.1 INTRODUCTION**

The Anterior Cruciate Ligament (ACL) is a set of two ligamentous connective tissue found in the knee binding the femur and the tibia, allowing the posterior translative movement and partial rotation of the limb. The ACL is present in a crucifix arrangement; with each of its individual ligament units, i.e. the anteromedial and posterolateral ligament, passing along the lines of the medial and lateral collateral ligament present behind the patella. The ACL is a part of the knee-joint system consisting of four different ligaments – the anterior cruciate ligament (ACL), the posterior cruciate ligament (PCL), the medial collateral ligament (MCL) and the lateral collateral ligament (LCL).

Tear of the ACL is one of the most common knee-related injuries in the world. It is estimated that up to 100,000 ligament tear injuries are reported annually in the US alone. The most common treatments to ACL tear includes the suture of torn ligaments, casting and immobilizing the injured area and replacement of ACL with the use of autologous or heterologous sources. Tissue grafting of the ligament is one of the most commonly reliable methods of ACL treatment. Ligament grafts are obtained either from the patient's own body (in which case it is known as Autologous tissue grafting) or from a non-self source such as a cadaver (in which case it is known as a heterologous tissue grafting). However, all these treatment methods have their own disadvantages such as inability of regeneration of the tissue at the site of trauma, secondary injury at the site from which the ligament graft was obtained (in case of autologous tissue grafting) or immune rejection of the tissue (in case of heterologous tissue graft) leading to failure of the grafting treatment.

Tissue engineering experiments were commenced for the fabrication of a suitable ligament tissue graft to overcome the aforementioned problems. Novel 3-dimensional scaffolds were synthesized using various natural and synthetic products in order to provide the mechanical support and strength for the growing ligament cells. However, it was later observed that the

ligaments grew well in-vitro and the formation of the tissue in laboratory conditions were perfect; nevertheless when the scaffold was transferred into the body to help the synthesized ligament implant within the knee, embedding itself within the tibia and femur, it was found that the tissue graft failed to integrate within the bones of the knee. Various reasons were brought into light for the failure of the experiments – early biodegradation of the scaffold, poor fixation of the scaffold at the site of injury, toxicity caused by the material of the scaffold etc.

One of the most important reasons for the above was found to be the failure of the ligament to reintegrate with the bones of the femur and tibia at the cellular and molecular level. Further studies revealed the presence of a specialized tissue which was comprised of fibrocartilaginous cells at the junction where the bone and the ligament meet. This tissue was called the Enthesis. Scientists realized that the failure of the tissue graft lied in the structural component of the artificial ligament where the enthesis was not present as a part of the organ. This led to further advancements in scaffold engineering experiments where the enthesis was included as an integral part of the scaffold along with the ligament and bone.

In the present project, we fabricate a knitted-silk-based scaffold which comprises of three compartments, one each for the bone, ligament and enthesis tissues. Each of these compartments are subject to surface modifications by using bio-polymers such as silk solution, chitosan, polyvinyl alcohol and hydroxyapatite on the appropriate compartments which help in the differentiation and development of Mesenchymal Stem Cells into their specific cell type i.e. the bone, ligament and fibrocartilage cells. We make use of various methods such as alternate soaking, plain coating and freeze-drying for the coating of polymers over the knitted silk. The scaffold is characterized for various properties such as

water absorption, biodegradability, tensile strength, purity of coatings, and biocompatibility.

## 1.2 Anatomy and Physiology of the ACL

The anterior cruciate ligament (ACL) (Figure-1) is one of the most important ligaments in the body. It is situated in the knee where it is notched into the femur, and it crosses the femoral chondyle and embeds itself deep within the tibia of the lower limb. Based on the structure and positioning of the ACL, it is also referred to as the Cranial Cruciate

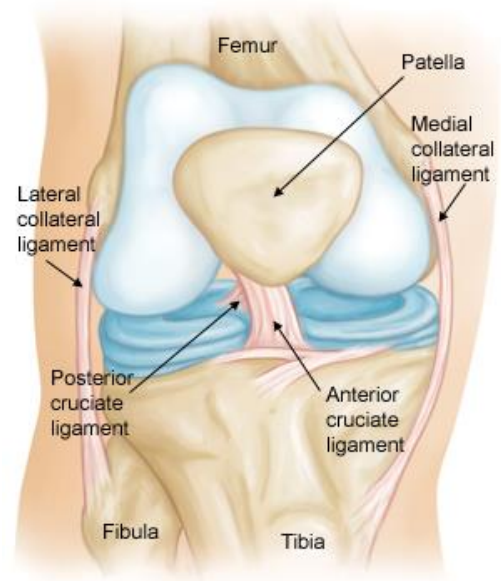


**Figure 1: Position of the ACL in the human knee**

Ligament [1]. The ACL is made up of the regular ligamentocytes present in the body

which function to stabilize the joint between two bones and provide them cushioning and prevent friction and abrasion between the bones [2]. The main function of the anterior cruciate ligament is to prevent the anterior translation and the medial rotation of the knee joint, which means that the knee is not allowed to move forward and rotate in its position, this major hindrance which is the most important property of the knee is provided by the ACL [3]. Hence it is unquestionably one of the most important ligaments in the knee region. Apart from the knee, the ACL is also present in the shoulder joint [4]. The ACL is adjoining other ligaments such as the posterior cruciate ligament, lateral collateral ligament and the medical collateral ligament which all help stabilize the structure of the knee [5,6,7]. The ACL is covered on top by the patella or the knee cap which prevents its exposure. The positioning of the ACL is such that it does not appear to be very rigid owing to its deep embedding within the femur and the tibia at the two ends, but also provides ample freedom of movement which helps in the one-directional movement of the knee as a whole [8,9].

This ligament is one of the most crucially examined region during knee injuries and is one of the most susceptible body parts for sports injuries and other medical hazards relating to the knee region. Hence it is a most closely studied ligament among all. [10]

### **1.3 Enthesis**

Enthesis is defined as that region of the body which forms a junction between a bone and a ligament [11,12,13]. This is one of the least known tissues of the body; however it is one of the most important regions when it comes to ligament tissue engineering and clinical ligament tissue graft replacement [14]. It is a small cartilaginous portion which is present at the junction where a bone and a ligament meet up. It is mainly composed of collagen type 1 and chondrocytes [15]. Depending on the position of the enthesis in the body, it can be classified to be of the following types:

- (i) Fibrocartilaginous: this type of enthesis is the most common type and is the most crucial type of tissue present at the anterior cruciate ligament. This type of enthesis is formed when the junction between a bone and a ligament is occupied by fibrous cells and they secrete their extracellular matrix in the surrounding region. Their thickness is varying depending on the site of their presence.
- (ii) Tendonous: this is the thickest type of enthesis present in the body. It is formed when the initial enthesis of the fibrocartilage origin matures and forms the tendon of the body. They are found mostly in the tendon region which connects a bone to a muscle.
- (iii) Calcified: at few regions, the enthesis tends to be calcified, especially when present at close proximity to the bone. They form a transition between the ligament/tendon towards the bone and forms a continuum between the two different tissue. [16-20]

Sometimes, it so happens that due to infection or complications of surgeries, the enthesis tends to develop lesions or get inflamed leading to its disintegration. These diseases which affect the enthesis are known as enthesopathies. During these times the joint between a

bone and ligament weakens and can lead to rupture or breakage of the bond leading to fractures or other injuries. Hence it is important that these damaged entheses be replaced by a possible tissue engineering methodology. These methodologies are also made use of during ligament damage and ligament replacement experiments.

Fibrocartilage type of enthesis is one of the most common types of enthesis in the body and hence are most preferred type of enthesis for tissue engineering experiments.

#### **1.4 Tissue Engineering for ACL regeneration**

During the damage of a ligament, it is mostly seen that the tissue samples are obtained from an exterior source, which is either an autologous source (the patient's own body) or from a cadaver or another species altogether. However many a times these surgeries and replacements of ligaments fail because the ligament which is fixed into a bone by drilling it within the bone cavity fails to form a reintegration joint with the bone. This leads to loosening of the bond between the two and ultimately failure of the graft. [21]

Scientists all over the world were perplexed as to the reason why a successful graft transfer surgery would fail within months, and the ligament would fail to establish to form a contact with the bone. It was after several close studies that a group of scientists discovered that though the ligament forms the connection between two bones, there was another tissue which formed the connection between a ligament and a bone too. This tissue which was later found to be fibrocartilaginous in nature was established as the enthesis tissue present in various ligament and tendons joints of the body. [22]

It was then that the scientists who were working on the preparation of a tissue graft and other tissue engineering experiments were made aware that preparation of just the ligament would not suffice, and that it was necessary that the enthesis tissue be engineered also along with the tendon so as to form an easy bonding between the bone and the ligament and help

speed up the reintegration process. For this purpose, various experiments were then carried out for the tissue engineering of the enthesis tissue. The various steps that were included in it were the fabrication of a suitable matrix to hold the cells, seeding of cells and growing them in a bioreactor providing suitable growth conditions for the ACL and other ligaments.

### **1.5 Objectives of Study**

In the light of the recent developments in ligament tissue engineering, numerous attempts have been carried out to fabricate the perfect scaffold for the growth and grafting of ligament cells. The current study proposes to fabricate a complex multi-compartmentalized scaffold which will support the growth of three different cell lineages (mature bone cells, ligament fibroblast and stem cells that can differentiate into cartilage) so as to tissue engineer a bone-ligament-bone graft *in vitro*.. Thus, the objective of the study is the fabrication of a knitted silk-based scaffold comprising of coatings of different biopolymers for different compartments which can support the mature cell lines (osteocytes, ligament fibroblasts) and/or induce the stem cells into cartilage cells. The objectives of the current project are elaborated below:

- 1.To fabricate a knitted-silk based multi-compartment scaffold for providing adequate mechanical strength to the proposed B-L-B graft.
- 2.To analyse the mechanical properties of raw knitted silk scaffolds in comparison with that of native ligament tissue.
- 3.To infuse compartment-specific biomaterial i.e. hydroxyapatite for bone, silk-chitosan blend for ligament and polyvinyl alcohol for fibrocartilage - over the knitted-silk scaffold.
- 4.To study investigate the biocompatibility of each biomaterial combinations through cell-attachment and cell-proliferation assays.



# **CHAPTER – 2**

## **LITERATURE REVIEW**

### 3.1 Ligament

Ligaments are known to be one of the few flexible tissues of the body, but also one of the most enduring ones. Depending on the location and the association of the ligament with other tissues, the mass and the functioning load of the tissue also varies. Ligament is the connective tissue which forms the connection between two bones. They are found all through the body and all bones, regardless of their bone, in the majority have the presence of ligaments within them. Among the most crucial of the ligaments is the Anterior Cruciate Ligament which is present at the condylar regions of the knee and the shoulder joints. The main function of the ACL along with the Posterior Cruciate Ligament is to restrict the directional and rotational movement of the joints in a single axis and one particular direction [22].

The histology of the ligament consists of ligamentocytes which are usually elongated in shape with a single nucleus, the extracellular matrix (ECM) and the fibroblast cells which are found freely within the extracellular matrix. The ligamentocytes are found in a uniform parallel arrangement and the cells communicate with each other through the formation of gap junction between each other with the help of extended cellular processes. Along with the main representative cells of a tissue, the fibroblast cells also help in the release of ECM in the form of collagen fibres and other molecules such as growth factors, adjuvants and paracrine signaling molecules. The main component of the ECM of the ligament is collagen Type I. The collagen molecules in the external environment of the ligament arrange themselves in parallel microfibrils which are closely enwrapped to form a characteristic tight binding macrofibre which provide the overall strength and endurance to the ligament tissue during the load bearing process. The ligament is not supplied with blood vessels and hence the nutrition to the organ is

provided by the components diffusing out of the blood vessels into the extracellular matrix which flow into the vicinity of the ligamentocytes.

### **3.2 Bone**

The bone is the strongest and one of the hardest tissues in the body. Due to its composition of calcium and phosphate minerals interlinked to form a hard hydroxyapatite compound, the strength of the bone is known to be phenomenal, along with the enamel minerals found in the teeth. This connective tissue forms the basic skeleton of the body, giving it shape and support to other organs to hold them in place and to facilitate the function of motion and movement. The histology of the bone consists of the basically three kinds of cells – the regular representative cells of the bone known as Osteocytes, the stem cell component of the tissue known as osteoblasts, and the macrophage-like cells of the bone which are responsible for the decay and disposal of dead bone cells and minerals, known as Osteoclasts [23]. The cells are surrounded by a mineral extracellular matrix mostly consisting of calcium-phosphate phase crystals known as hydroxyapatite.

The connection and the communication of cells within the tissue and with that of the ones outside are carried out by micro-channels, usually known as Harvesian canals, which carry the nutritional components towards the various cells of the bone. There are other micro-channels which interconnect the cells to one another within the mineral matrix, the principles of the flow of materials through these channels and the study of their effect on the cells are all investigated as part of microfluidics branch of research.

The bones are connected to each other via ligaments and to that of the muscle via tendons. The joints between two bones where movement is involved are usually articulate in nature with the arrangement of ball-and-socket architecture which facilitates the

movement of two bones onto each other. The ligament usually integrates deep within the bone, embedded at the point of contact between the two tissues [24].

### **3.3 Enthesis**

Enthesis is the junction tissue at the point where the bone meets the ligament. It is composed of fibrocartilage tissue which contains collagen type 1 as seen in the ligament. However, unlike the ligament and other tissues where collagen is present, the collagen in the enthesis fibrocartilage is haphazard in nature and non-uniform in alignment. This, while making the enthesis not fit for high load bearing, it also makes the tissue strong enough to form the bond between the two load bearing tissues and hence integrate the two to conform to its ideal tensile enthrusting structure [25].

Categorically there are three types of enthesis tissues – the fibrocartilage enthesis, the tendonous and the tidemark region. These forms of enthesis are basically classified based on their structure and they are not necessarily found in different regions of the body, but more like found as transition from one form to the other in the same tissue region. At the junction between the bone and the ligament, the enthesis starts out as a ligamentous form where the arrangement of collagen type I are parallel to each other forming a tight bond, as the enthesis progresses towards the bone it becomes more cartilaginous in nature with the presence of fibroblast cells releasing their fibrous extracellular matrix which have irregular collagen fibres which do not give rise to any principled structure; and at the point of infusion of the bone and the enthesis is where the calcification of the enthesis can be found. This is seen as a mere attempt to make the enthesis more compatible with the changing tissue type with the deposition of calcium minerals in the extracellular matrix. There are various diseases associated with the enthesis malfunction which subjects a

patient to joint impairments or makes a person susceptible to injuries with even a very low impact. These diseases are diversely known as the Enthesitis or Enthesopathies [26].

### **3.4 Enthesis tissue engineering**

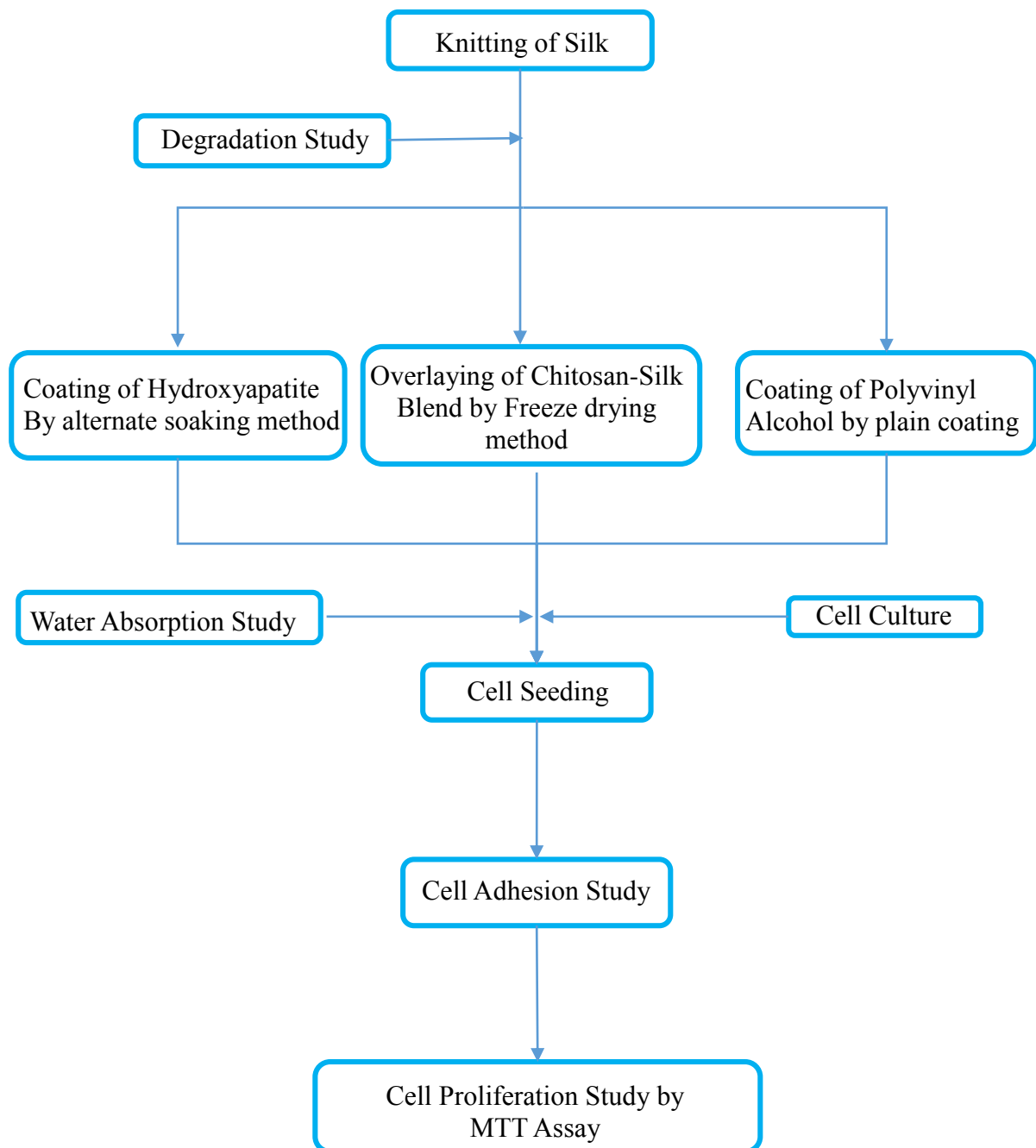
Ligament tissue engineering has been one of the most sought after tissue engineering ventures in the scientific fraternity which deals with the fabrication of artificial organs and tissues. The susceptibility of the ligament towards injury and the fact that the regeneration of the organ happens anything but accurate, it is known to be a very suitable candidate for the possibilities of new dimensions of inventions and discoveries. The poor quality of regeneration of the ligament is usually associated with the fact that the tissue is not supplied with blood vessels, owing to which it does not receive the necessary conditions and growth factors after injury that can lead to its effective regeneration. Also, the presence of ligament stem cells is seen to be very low, which also contributes to this malady [27].

The fabrication of a scaffold for ligament tissue engineering has been sought after various scientists in the regenerative medicine domain. A number of biomaterials including natural and synthetic products have been used for the preparation of these scaffolds. The scaffolds are usually furnished in 2-D form with the prospect that they can be fabricated in 3-D form once the growth and sustenance of the cells can be established on them. Apart from scaffold technology, there have been other methods where the ligament injury has been treated, like the suturing of heterograft or xenograft ligaments on the body of the patient, or the attachment of an autologous graft using body-implantable noble metal screws and harnesses [28]. However, the experiments have seen little light of success during the formation stage of the tissue on the scaffold or in the implantation stage where the ligament is supposed to reintegrate with the tissue of the bone. The failure was at first

not seen closely. Scientists later discovered that the failure of the ligament tissue integration was imminent because every time a ligament graft was prepared, experimentalists often overlooked a key cellular system which was present at the junction of the bone and the ligament. This tissue, which is called the enthesis, has now found great interest in the scientific world where the tissue engineering of joints is involved. The presence of this tissue in the integration stage is seen as a key step to the total molding of the tissue to the skeletal system [29,30]. Scientists have now started testing their success in the fabrication of scaffolds where apart from the bone and the ligament, the enthesis tissue is also supported for the growth. Scaffolds are now being prepared which include sections for the growth of enthesis fibrocartilage cells. The scaffold system varies either in the form that separate scaffold entities are first designed, cells are impregnated and allowed to grow on them and then the scaffolds are sutured together to give a combination scaffold of different cellular system, or in few cases scientists have had success in devising scaffolds where a single scaffold is divided into different compartments where different variety of cells are implanted and the nature of their growth, interaction with each other and the maturation of stem cells to form their representative mature tissue cells are examined [31]. The success of an ideal scaffold is where the stem cells obtained from the bone marrow (mesenchymal in nature) are able to mature and differentiate into their mature counterparts such as the ligamentocytes, osteocytes and chondrocytes while interacting with each other and while growing on the scaffold matrix material and can give rise to a full mature tissue type consisting of all the three components and which can be biocompatible in an animal model study and finally at the clinical stage where it can be implanted within the body for a fully functional ligament, while also degrading within the body to be excreted easily from the systemic fluid without giving rise to any cytotoxic repercussions [32].

# **CHAPTER – 3**

## **PLAN OF WORK**





# **CHAPTER – 4**

## **MATERIALS AND METHODS**

## **4.1 FABRICATION OF SCAFFOLD**

### **4.1.1 Preparation of Silk Yarn**

Silk fibers were procured from Raw Tasar Silk Depot, Chiabasa, Jharkhand, India. Out of the many types of silk fibers that were procured, the silk strand having 12 fibers was made use of. The fibroin was stretched and woven around to form a 12-threaded yarn which was then braided to result in a cluster thread of roughly 2mm thickness. This silk thread was used further to prepare the knitted-silk base for the scaffold.

### **4.1.2 Knitting of Silk**

The woven silk fibroin threads were used to make yarns which were knitted using Brother Knitting Machine (Model no. KH830) using 6 alternative needles to obtain a patterned mesh of dimension 2cmX6cm with preset pore patterns. To carry out the knitting, six alternate needles were pushed to 'Out' position. The yarn threads were loaded to K-carriage and pulled towards the right end. The six needles were shifted to 'Working' position. The 'Claw' weights were used to provide uniform force towards the ground during knitting process to direct the knitted silk downwards. The K-carriage was alternatively slid left and right over the six needles to commence the knitting process. Once knitting was completed, the remaining yarn was cut about 10cm from the main knitted silk and the K-carriage was moved away from the knitted silk. The knitted mesh was then tied on to a rectangular glass slide of dimension 3cmX8cm such that the mesh is exposed on one side of the glass slide or rimmed with metal wire which can be used for coating of polymers and cell seeding during later experiments; and extensions of the thread flanking from either sides of the mesh were used to tie a knot behind the glass slide to keep the silk mesh intact in its position. This constituted of the knitted-silk base which was used for all subsequent experiments (Figure 2).

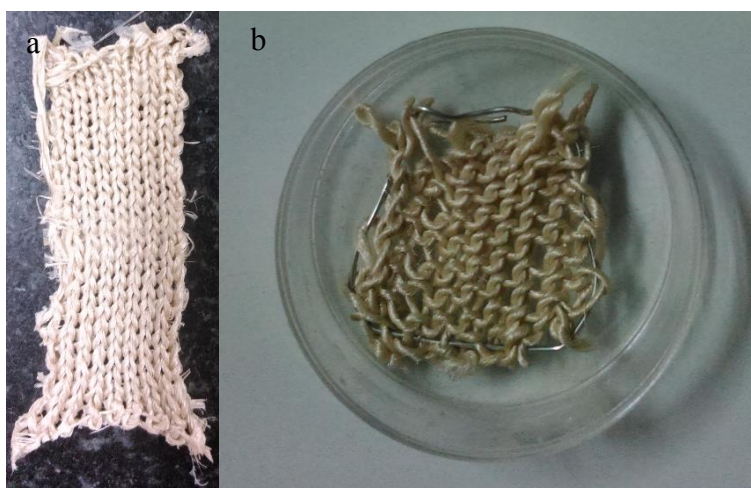


**Figure 2: Knitted Silk scaffold fixed on (a) glass slide (b) wire frame**

#### **4.1.3 Morphological Characterization of Knitted Silk**

The morphological characterization of the knitted silk base was carried out in FEI-NovaSEM 450 field emission scanning electron microscope using gold coating. The knitted silk was cut into small square pieces of dimensions suitable to load on the sample holder of the device. The fibers were subjected to sputter coating of gold for 2 minutes prior to visualization of the same under the microscope. The knitted silk was observed under an electric field of 20KV and was visualized at 30x magnification.

#### **4.1.4 Preparation of Phosphate Buffered Saline**

Phosphate Buffered Saline (PBS) is one of the most important buffers used in vitro studies and for preparation of experimental solutions, due to its constituent and parametric resemblance to the body fluids. 1L of 1X PBS solution was prepared. 8g of NaCl was mixed thoroughly followed by 0.2g of KCl. This was followed by the addition of 1.44g of  $\text{Na}_2\text{HPO}_4$  and then  $\text{KH}_2\text{PO}_4$ . The pH of the solution was adjusted using 1N NaOH and 1N HCl until the value was set at 7 at 25°C.

#### **4.1.5 Mechanical Strength Testing**

The study of mechanical tensile strength of a scaffold is one of the key parameters in the design of an ideal scaffold. The objective of the study is to make sure that the scaffold is strong enough to bear mechanical load in regions that it is implanted. Additionally it also gives an idea of the degradation rate of the scaffold when present in an environment of body fluids.

The knitted-silk meshes were immersed in 1X Phosphate Buffer Saline (PBS) adjusted to pH-7 at 37°C for a duration of 3, 7, 14, 21 and 31 days. The pH of the buffer was adjusted using 1N HCl and 1N NaOH solutions as per requirements. Once the stipulated time was completed for each knitted-silk mesh, it was taken out of the buffer solution, dried and tested for mechanical tensile strength using TA-HD Plus Texture Analyser where the gauge length was set at 20mm and cross head speed was maintained at 10 mm/min uniformly for all the meshes.

### **4.2 POLYMER COATING OF KNITTED-SILK SCAFFOLD**

#### **4.2.1 Preparation of Silk Solution**

Silk solution was prepared using raw silk cocoons of *Bombyx mori* silkworm. The cocoons were first cut into two halves and the carcass of the worm along with any dirt or impurity was removed. The cocoons were then cut into very fine pieces boiled in degumming solution for 3 hours with regular change of the solution every half an hour. The degumming solution, which is made of 2% (w/v) Na<sub>2</sub>CO<sub>3</sub> dissolved in distilled water, is basically used to remove the antigenic sereccin from the silk fibroin so as to prevent immunogenic response once the final scaffold is implanted into the body. Once the cocoons are boiled in the degumming solution, they are removed and washed in running distilled water close to 20 minutes and air dried overnight. The dry degummed silk fibres are then dissolved in

98% formic acid solution at room temperature at different concentrations (w/v) as per requirement of the experiment. The silk fibres were stirred overnight at room temperature for complete dissolution in the solvent.

#### **4.2.2 Alternate Soaking Process - Hydroxyapatite**

120mM solution of  $K_2PHO_4$  was prepared in 0.1M Tris base solution. This solution was called Solution-A. 200mM solution of  $CaCl_2$  was prepared in the same buffer and called Solution-B. The partially covered knitted scaffolds were first immersed completely in solution A for 30 minutes, then removed from the solution and was blotted for excess solution before immersing it in solution B for the same duration. Likewise they were alternately immersed completely in both these solution for a total of 20 cycles. The scaffolds after 5, 10, 15 and 20 cycles of alternate soaking were respectively chosen as principal samples for further studies. The samples were then subjected to serial dehydration by immersing them in ethanol solutions of increasing concentration – 30%, 50% 70% and 100% (all percentages are in v/v ratio). These scaffolds were then sealed in airtight containers and stored until they were used for further analysis and other experiments (Figure 3).

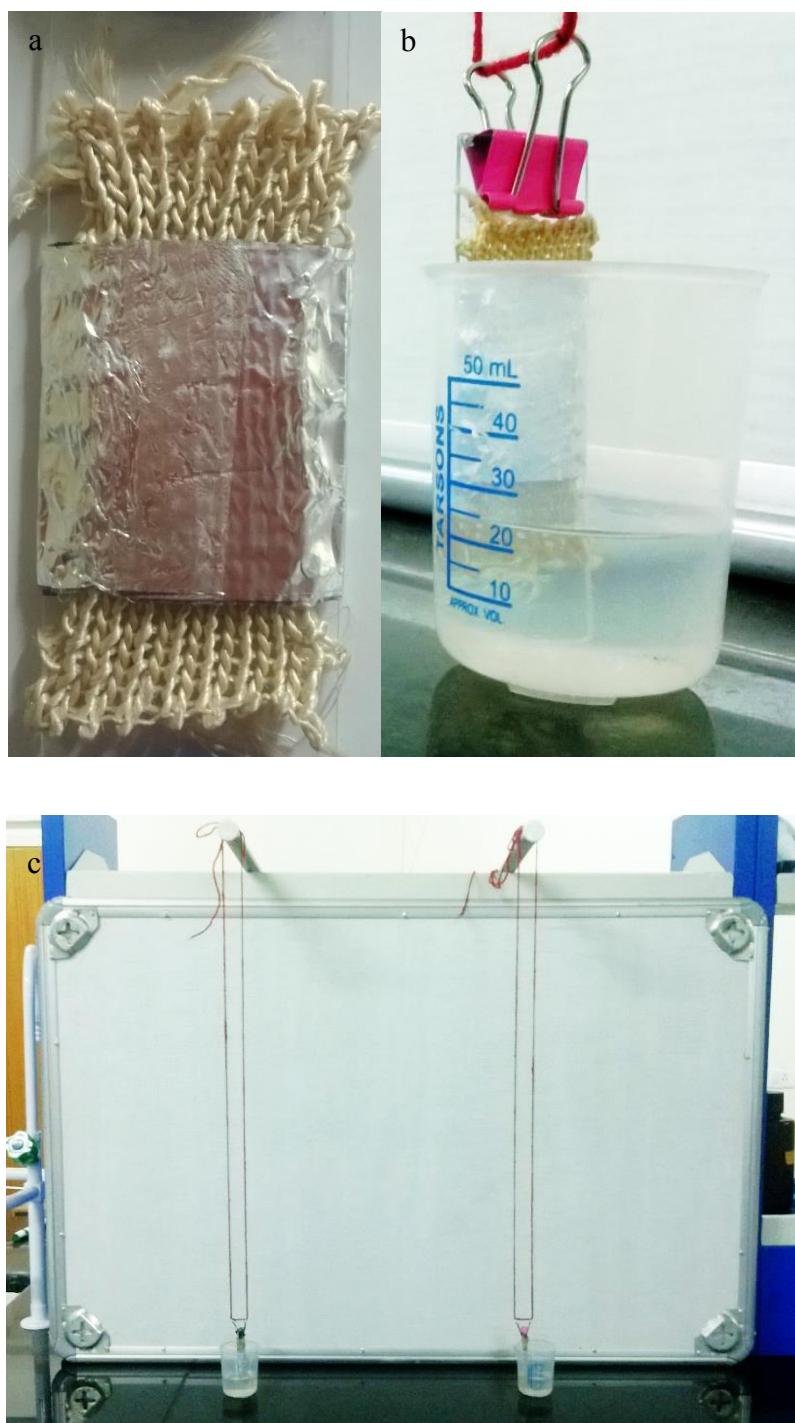


**Figure 3: Experimental setup of Alternate Soaking process for Hydroxyapatite coating on knitted silk based scaffold. (a) Preparation of the knitted silk scaffold for hydroxyapatite coating. (b)(c) Alternate soaking in the two solutions.**

#### 4.2.3 Freeze Drying Process – Silk/Chitosan Blend

Silk/chitosan blend solutions were prepared by dissolving equal amounts of silk and chitosan in 98% (v/v) formic acid and 2% (v/v) acetic acid respectively. Both silk and chitosan were added in increasing amounts – 2%, 4%, 6%, 8% (w/v) - in their respective solvents stirred at 60°C until all the particulates have dissolved in the solvent. The solutions of the two polymers were mixed together such that the resultant solution contained equal concentration of both silk and chitosan. Knitted-silk fibers were immersed into these solutions and subject to lyophilisation to remove the solvent molecules resulting in the coating of silk-chitosan blend over knitted silk base (Figure 4).

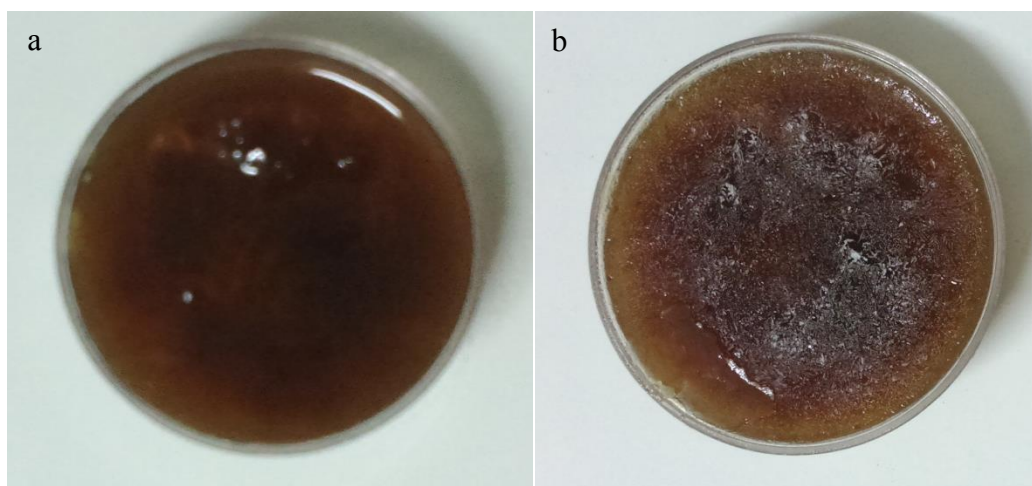


**Figure 4: Silk/Chitosan Blended solution for sponge overlaying on knitted silk based scaffold (a) before freezing (b) after freezing**

#### 4.2.4 Plain Coating – Polyvinyl Alcohol

Polyvinyl alcohol (PVA) solutions of different concentrations - 4%, 6%, 8%, 12% (w/v) - were prepared by dissolving the respective quantity of PVA powder in distilled water and stirred at 60°C for up to 4 hours during which the powder completely dissolves in the water solvent. Knitted silk fibers were immersed into the solutions of PVA and subject to air

drying at room temperature for up to 6 hours, until a dry layer of PVA over the silk fibers is observed.

### **4.3 CHARACTERIZATION STUDIES**

#### **4.3.1 Water Absorption Studies**

Water absorption properties were studied for each type of scaffold. PBS solution was prepared at pH 7. Initial dry weights of all three scaffolds noted and then they were immersed in PBS at 37°C (denoted as  $W_0$ ). The weights of scaffolds was monitored every 60 minutes and was immersed back in fresh PBS solution under the same conditions. The newly acquired weights were noted until there was no recurrent change in the weight of the sample (final weight denoted as  $W_n$  where 'n' the last immersion step). This was assumed to be the maximum absorption capacity of the scaffold. The water absorption percentage of the scaffold was calculated using the following formula:

$$\% \text{ Absorption} = \frac{W_n - W_0}{W_0} \times 100$$

The absorption capacity of water depends upon the affinity of the scaffold material over with water molecules and the size of the scaffold. Keeping this in mind, the absorption study was carried out keeping all the sizes of each category of scaffold same among themselves. Hydroxyapatite coated scaffolds were studied using a uniform size of 60mm X 20mm dimensions. Silk/Chitosan scaffolds and PVA coated scaffolds were kept at a uniform dimension of 30mm X 20mm.

#### **4.3.2 Field Emission Scanning Electron Microscopy (FE-SEM)**

Topology study of the hydroxyapatite-coated scaffold was carried out using FEI-NanoNovaSEM 450 field emission scanning electron microscope. The four main sample scaffolds of alternate-soaking experiment were cut in appropriate dimensions and sputter



coated under vacuum with particulate gold for a duration of 2 minutes. The scaffolds were then shifted to high vacuum chamber of the FE-SEM and were visually observed for their characteristics at magnifications of 100X, 500X, 2000X and 25000X.

#### **4.3.3 Fourier Transform Infrared Spectroscopy (FTIR)**

Fourier Transform Infrared Spectroscopy was performed for the hydroxyapatite-coated samples. It was carried out using IR Prestige-21 FTIR Spectroscopy, Shimadzu Corp. (Japan). The samples were cut into very fine pieces, and pressed into pellets and placed on the sample holder. The IR peaks for the scaffold coated with different concentrations of hydroxyapatite were obtained.

#### **4.3.4 X-Ray Diffraction (XRD)**

X-Ray Diffraction studies were performed for all three kinds of scaffolds – hydroxyapatite coated, silk/chitosan coated and PVA coated – with different concentrations of coatings. XRD was carried out using Rigaku Ultima IV X-Ray Diffractometer at an observational range of 10°-60° with a step size of 0.04° and at a rate of 3°/min. An energy of 2kW under 60kV was supplied to A-41-Copper electrodes emitting beams through a window of 10mm width.

### **4.4 BIOCOMPATIBILITY STUDIES**

For the study of cell attachment and cell proliferation on the different types of coatings on the knitted silk, two types of cells were used, both procured from National Centre for Cell Science, Pune. Saos-2, an osteoblast-like cell line isolated from human primary osteosarcoma, was used to study the osteoconductive properties of hydroxyapatite coating on the scaffold. MG-63, a fibroblastic cell line derived from human primary osteosarcoma, was used to study the attachment and proliferative properties of silk-chitosan blend and PVA coating on the knitted silk.

#### 4.4.1 Cell Culture

The culturing and incubation protocols followed for both Saos-2 and MG-63 cell lines were identical. The cells were cultured using DMEM-Low Glucose growth media (Himedia, India) and supplemented with 5% (v/v) fetal bovine serum in a T-75 culture flask. The media was replaced every 48 hours. The culture flasks were periodically examined for proliferation and confluence. Once the cells reached 80% confluence, they were subjected to sub-culture. Subculture was carried out by initially removing the media from the flask, and subsequent washing of the cells with PBS. This was followed by trypsin treatment where trypsin-varsene solution was washed over the cells and incubated at 37°C for 2 minutes to detach the cells from the surface of T-flask. They were then washed using DMEM containing FBS to inactivate the enzymatic action of trypsin. The cells, which are now suspended in the latter solution, are subjected to centrifugation at 8000rpm for 5 minutes wherein the cells settled to a pellet at the bottom of the centrifuge vial. The cell pellets were collected and their concentration was calculated using a Neuber's Chamber. The cells were then appropriately distributed into new flasks in 1:4 ratio as recommended by NCCS Pune.

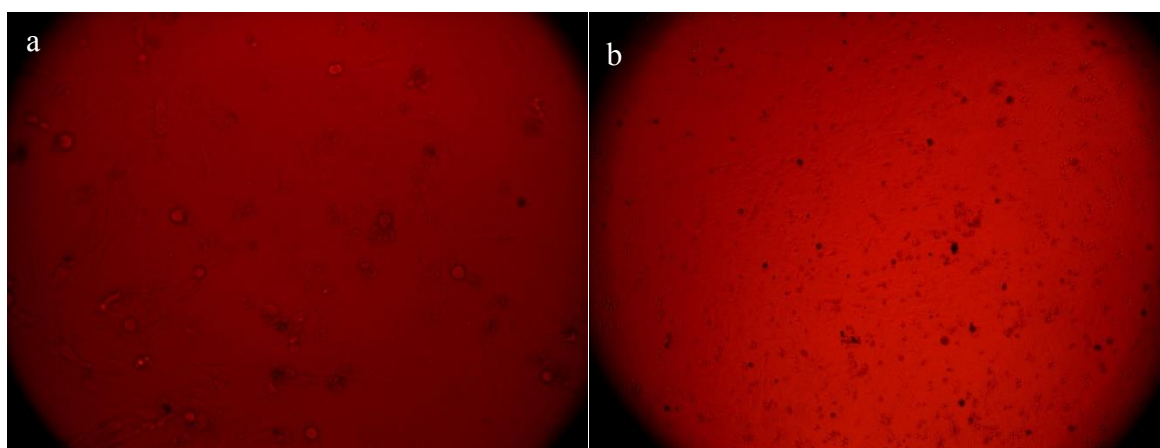


**Figure 5: Cells used in the experiment (i) MG-63 and (ii) Saos-2**

#### **4.4.2 Scaffold Sterilization**

The scaffolds were placed in 100mm<sup>2</sup> Petri-dishes, placed inside the biosafety-cabinet and subjected to formaldehyde fumigation. Formaldehyde solution (37%) was kept in another Petri-dish and kept inside the biosafety cabinet along with the scaffolds such that the vapours of formaldehyde penetrate the scaffolds and decontaminate them. This was followed by exposure of scaffolds to UV light for 5-10 minutes and washing with PBS thrice to remove traces of formaldehyde from within the scaffold. The scaffolds were then stored in sterilized desiccator until further use.

#### **4.4.3 Cell Seeding**

Cell seeding was carried using regular cell-drop method where cells in media at a concentration of  $2.8 \times 10^6$  cells/ml (MG-63) and  $2.3 \times 10^6$  cells/ml (Saos-2) was seeded over the scaffolds. After an interval of 60 minutes, DMEM supplemented with 5% fetal bovine serum was added to the scaffold. MG-63 cells were seeded over hydroxyapatite-coated scaffold while Saos-2 cells were seeded over silk-chitosan blend and PVA coated scaffolds.

#### **4.4.4 Cell Adhesion Study**

To find out the concentration of cells attached to the surface of the scaffold, 30mm X 20mm pieces of each scaffold sample (including that of different concentrations of coatings) was used. Cell seeding was performed at a concentration of  $2.8 \times 10^6$  cells/ml (MG-63) and  $2.3 \times 10^6$  cells/ml (Saos-2) as mentioned above and incubated in CO<sub>2</sub> incubator. After 24 hours, the scaffolds were removed from the petri-plates and the media was collected in 15 ml tubes. Further, the petri plates were subjected to trypsin treatment and then washed with media supplemented with serum to dislodge any cells attached to the surface of the petri plate and transferred to same tubes. The washed media was subjected to

centrifugation at 8000rpm for 5 minutes and cell count of the pellet was carried out. This cell concentration was subtracted from the initial cell seeding concentration to obtain the number of cells attached to the surface of the scaffold.

#### **4.4.5 Cell Proliferation Study**

MTT assay was carried out to study the cell proliferation over the scaffold. Briefly, MTT solution was added to the cell seeded scaffold bearing culture media at 4 $\mu$ l/100 $\mu$ l concentration along with a sample of plain media (control), and incubated at 37°C for 30 minutes. Next, formazan was solubilized using 3ml acidic isopropanol solution. The solution was pipetted repeatedly and incubated at 37°C for 30 minutes to ensure complete dissolution of formazan. Optical density (OD) of the resulting solution was checked at 540nm. Serial dilutions of a known cell concentrate was processed by method described above to obtain a standard plot (OD against cell concentrations). Absolute cell number was counted for studying cell proliferation by matching the ODs in the standard plot.

#### **4.5 FABRICATION OF HYBRID SCAFFOLD**

With conclusions drawn on the results of the above experiments, an ideal scaffold was fabricated by combining the best results of water absorption, cell proliferation and cell attachment studied for each concentration of the 3 polymers, i.e. hydroxyapatite, silk/chitosan and PVA. These best concentrations of each polymer/combination were then integrated into a single knitted-silk of 6mm X 2mm dimension to obtain an ideal Bone-(entheses)-Ligament-(entheses)-Bone scaffold. The water absorption capability, cell adhesion and cell proliferation studies were performed on the hybrid scaffold to yield its ideal properties.

# **CHAPTER - 5**

## **RESULTS AND DISCUSSION**

## 5.1 MORPHOLOGY OF SCAFFOLD

### 5.1.1 Morphology of Knitted Scaffold

The morphology of the knitted silk scaffold, which was prepared by knitting 12-yarn silk fibres (Brother Knitting Machine, China), was observed at 30X under FE-SEM. The image shows uniformly knit loops of silk fibres coiled around each other to form a mesh of consistent thickness and interconnectivity. The average pore size of each loop of the knit was found to be around 1mm. A cluster of 12 individual fibres of the yarn looped around each other to render a firm gripped thread can be clearly distinguished in the image (Figure 6).

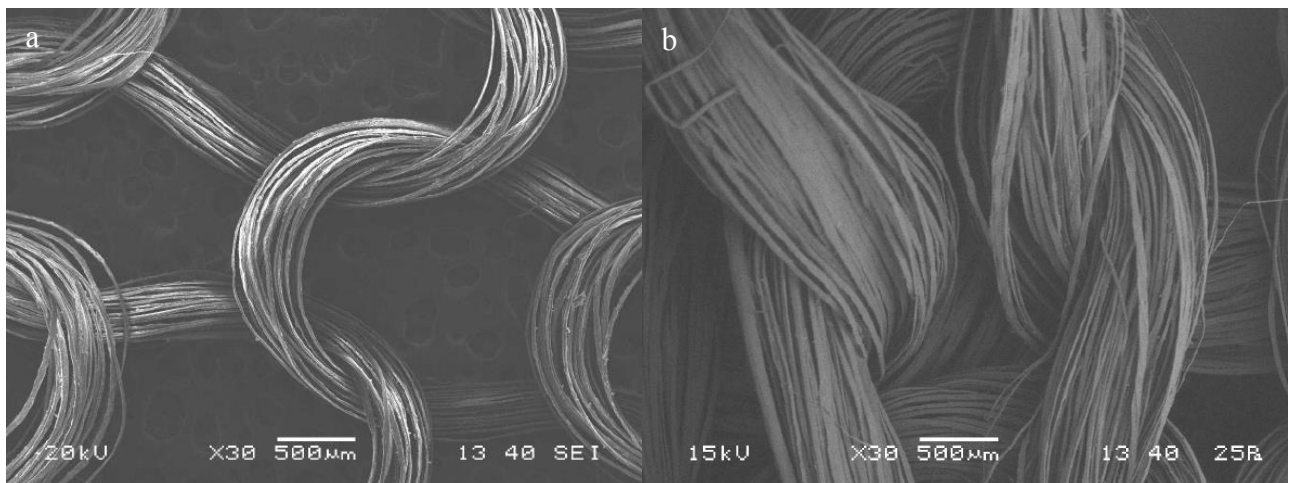


**Figure 6: Morphological visualization of knitted silk based scaffold under SEM**

### 5.1.2 Morphology of Hydroxyapatite Coating

Hydroxyapatite coating over knitted silk scaffold was carried out by soaking the silk fibres alternately in solutions of  $K_2HPO_4$  and  $CaCl_2$ . The thickness of the scaffold, as observed by the naked eye (Figure 7), increased with the increasing number of cycles of immersion in the two solutions. The flexibility of the scaffolds also decreased with increasing coating cycle due to more deposition of hydroxyapatite over the knitted silk.



**Figure 7: Knitted silk scaffold after alternate soaking of hydroxyapatite (10 cycles)**

#### **5.1.2.1 SEM Analysis of Hydroxyapatite Coating**

SEM analysis revealed that hydroxyapatite coating was present uniformly throughout the scaffold and around each strand of the fibre. With increasing cycles of soaking, the gap between the fibres of the knitted silk reduced. The thickness of each strand of silk was about 52 $\mu$ m and that of each fibre of the yarn was 585  $\mu$ m in the first sample of 5 cycles of alternate soaking. The corresponding values increased to 131  $\mu$ m and 921  $\mu$ m of the counterpart with 20 cycles of the alternate soaking process.

It was also observed that the morphology of the hydroxyapatite coating over the scaffold was quite unique. As compared to earlier literature which claimed the presence of nano-scale spherical bead-like morphology of the mineral, this study revealed the presence of polygonal flake-like hydroxyapatite coating which were close to 500nm in breadth Figure 8-11 show the SEM representations of hydroxyapatite coated silk fibres in varying magnifications when the alternate soaking process was carried out serially for 5, 10, 15 and 20 cycles respectively.

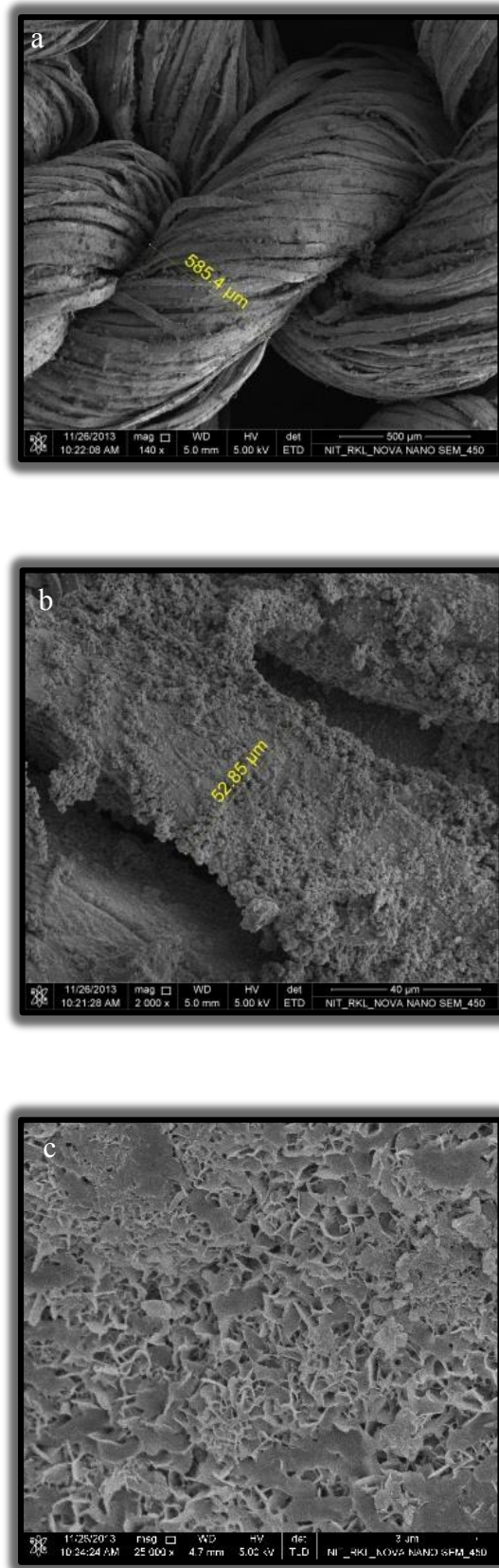


**Figure 8: SEM micrograph of hydroxyapatite coated knitted silk based scaffold after 5 cycles of alternate soaking process in (a) 500X, (b) 2000X and (c) 25000X magnifications**



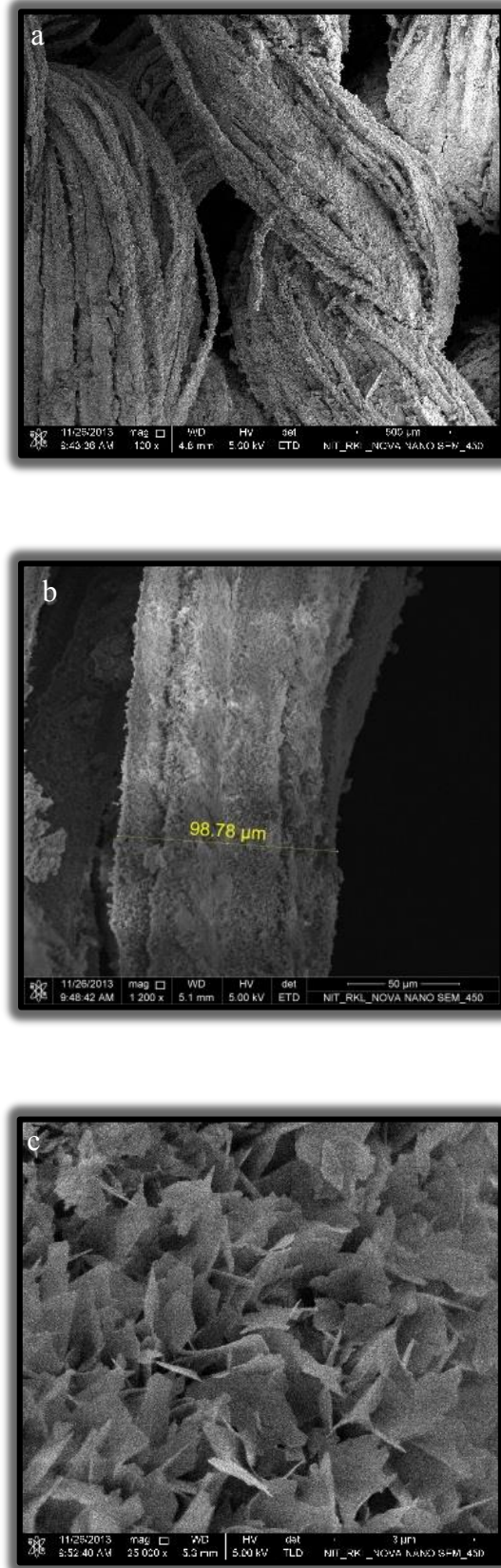


**Figure 9: SEM micrograph of hydroxyapatite coated knitted silk based scaffold after 10 cycles of alternate soaking process in (a) 500X, (b) 2000X and (c) 25000X magnifications**

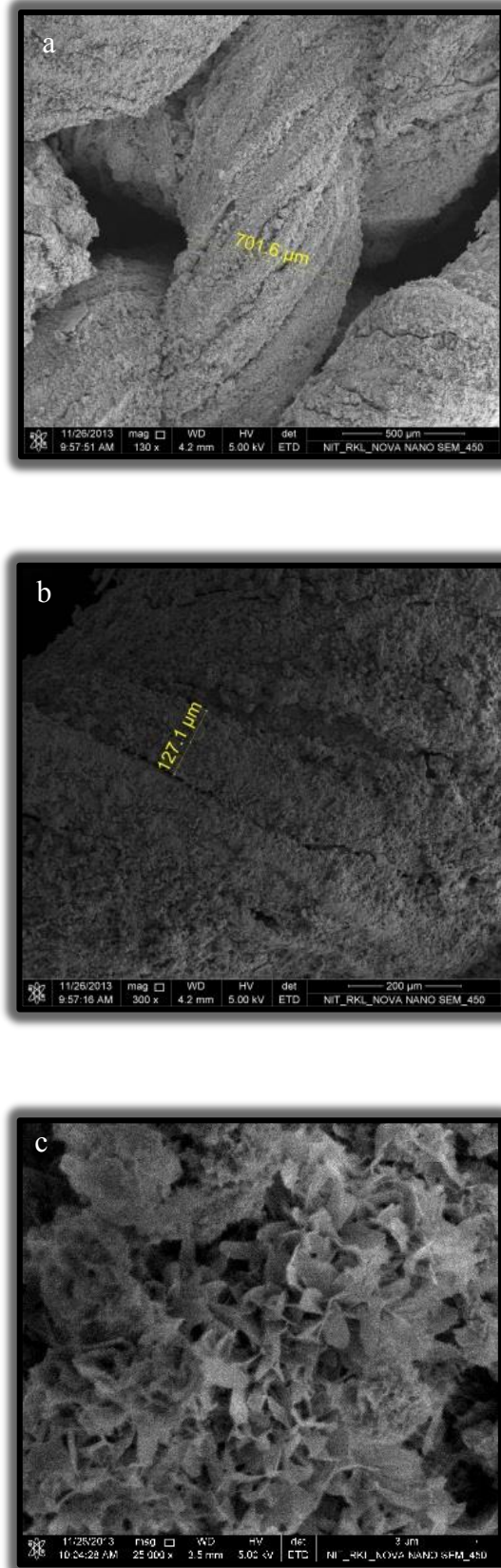


**Figure 10: SEM micrograph of hydroxyapatite coated knitted silk based scaffold after 15 cycles of alternate soaking process in (a) 500X, (b) 2000X and (c) 25000X magnifications**

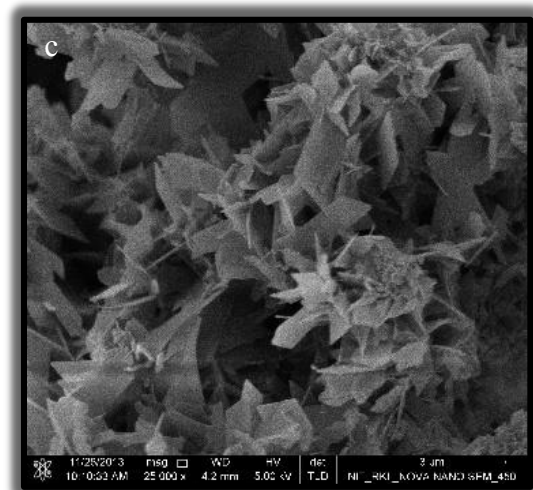
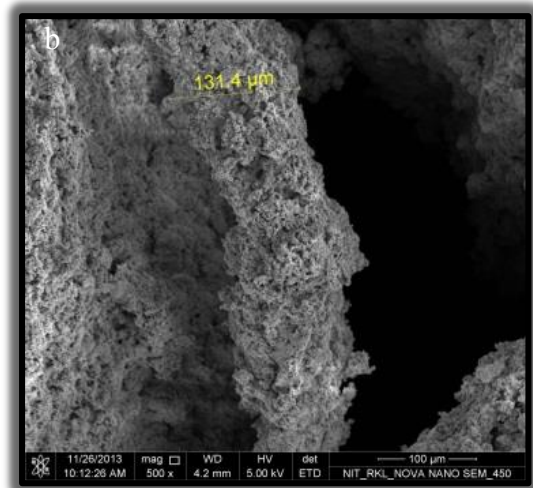
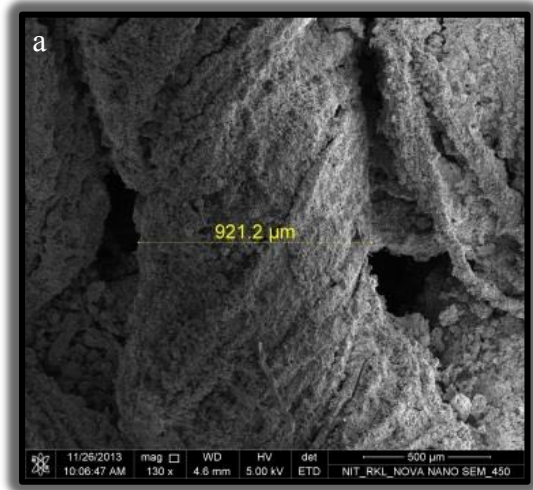


**Figure 11: SEM micrograph of hydroxyapatite coated knitted silk based scaffold after 20 cycles of alternate soaking process in (a) 500X, (b) 2000X and (c) 25000X magnifications**

### 5.1.2.2 XRD Analysis of Hydroxyapatite Coating

XRD analysis was carried out to understand the crystallinity of the hydroxyapatite coating formed on the knitted scaffold. Peak intensities around  $2\theta$  values of  $32^\circ$  and  $26^\circ$  are indicative of the presence of hydroxyapatite crystals. The sharpness of the peak indicated the fine crystallinity of the hydroxyapatites formed on the knitted silk scaffold. Figure 12 shows the characteristic XRD peaks of the mineral.

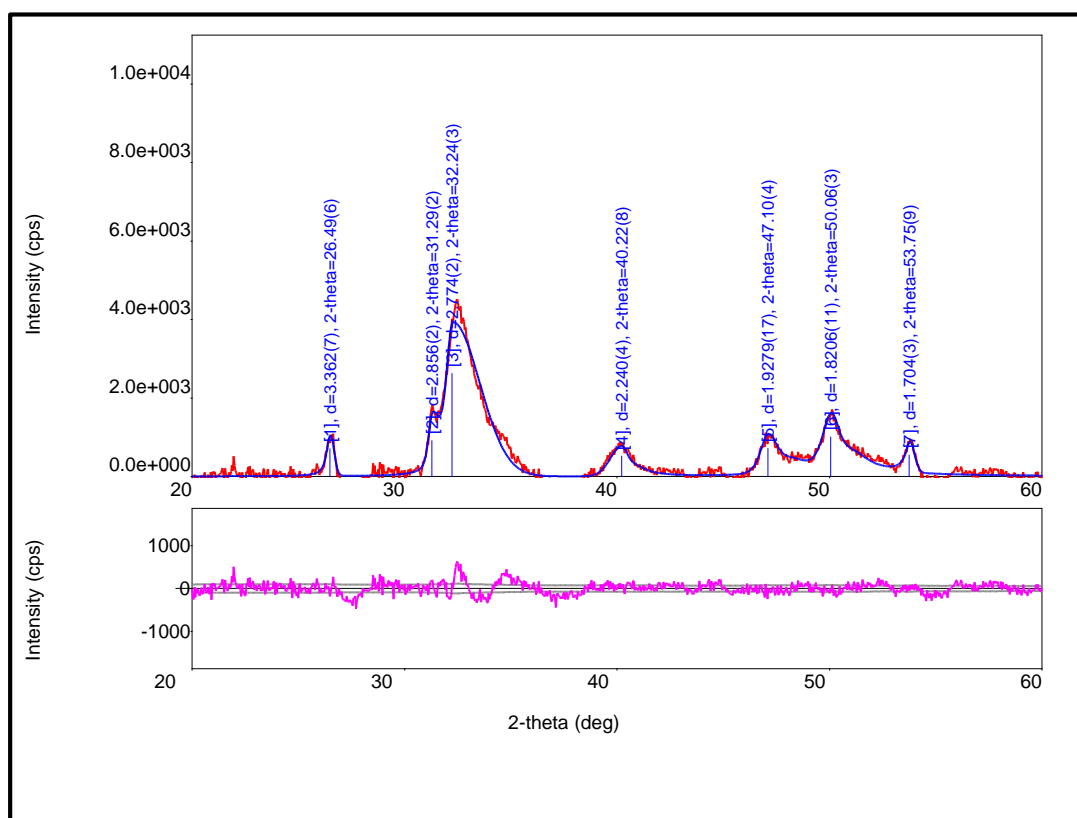
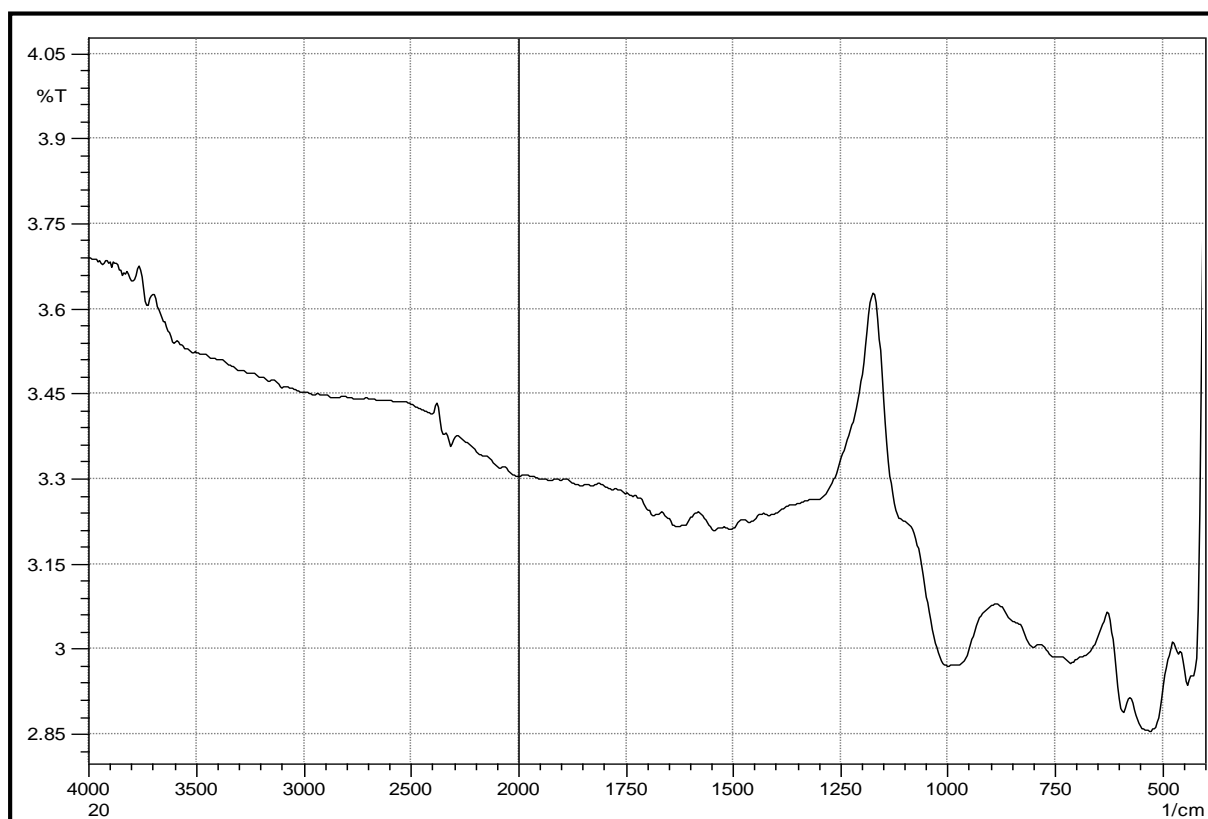


Figure 12: XRD of alternate soaking experiment showing representative peaks of HA crystals on knitted silk based scaffold

### 5.1.2.3 FTIR Analysis of Hydroxyapatite Coating

FTIR analysis was carried out to determine the bond characteristics and the side chains present in the sample. The major peak at around  $1250\text{ cm}^{-1}$  is indicative of the presence of amide III linkage of silk fibroin. The peaks around  $604\text{ cm}^{-1}$  and  $565\text{ cm}^{-1}$  are indicative of

$\nu_4 \text{PO}_4^{3-}$  present in apatite. Peaks around  $962 \text{ cm}^{-1}$  indicate  $\nu_3 \text{PO}_4^{3-}$  and peak around  $530 \text{ cm}^{-1}$  represent  $\text{HPO}_4^{2-}$  of the apatite mineral (Figure 13).



**Figure 13: FTIR analysis of alternate soaking process showing representative peaks of HA on knitted silk based scaffold**

### 5.1.3 Morphology of Silk/Chitosan Sponge

Silk/Chitosan blend scaffold was prepared by preparing a solution containing mixture of equal concentrations of both silk and chitosan, and subjecting the solution to freeze drying. Freeze drying facilitates the evaporation of the volatile content of the solution by first freezing it and lowering the pressure down to vacuum conditions, in turn converting the solid solvent directly into vapour, in a process known as sublimation.

Silk/Chitosan layered over knitted silk scaffold appeared as smooth sponges once the solvent was removed. Depending on the concentration of silk/scaffold in their respective solutions, the colour of the solution varied from brownish yellow for 2% solution of both



silk and chitosan mixed together; to blackish brown in solution containing 8% of both silk and chitosan. Since the sponges were smooth in nature, the hardness of the material did not vary much with increasing concentration of the individual components. The scaffold was prone to formation of cracks upon flexing and bending of the scaffold, due to the brittle nature of the sponge. Figure 14 shows the characteristic appearance of silk/chitosan blended lyophilized sponges in their increasing concentrations.

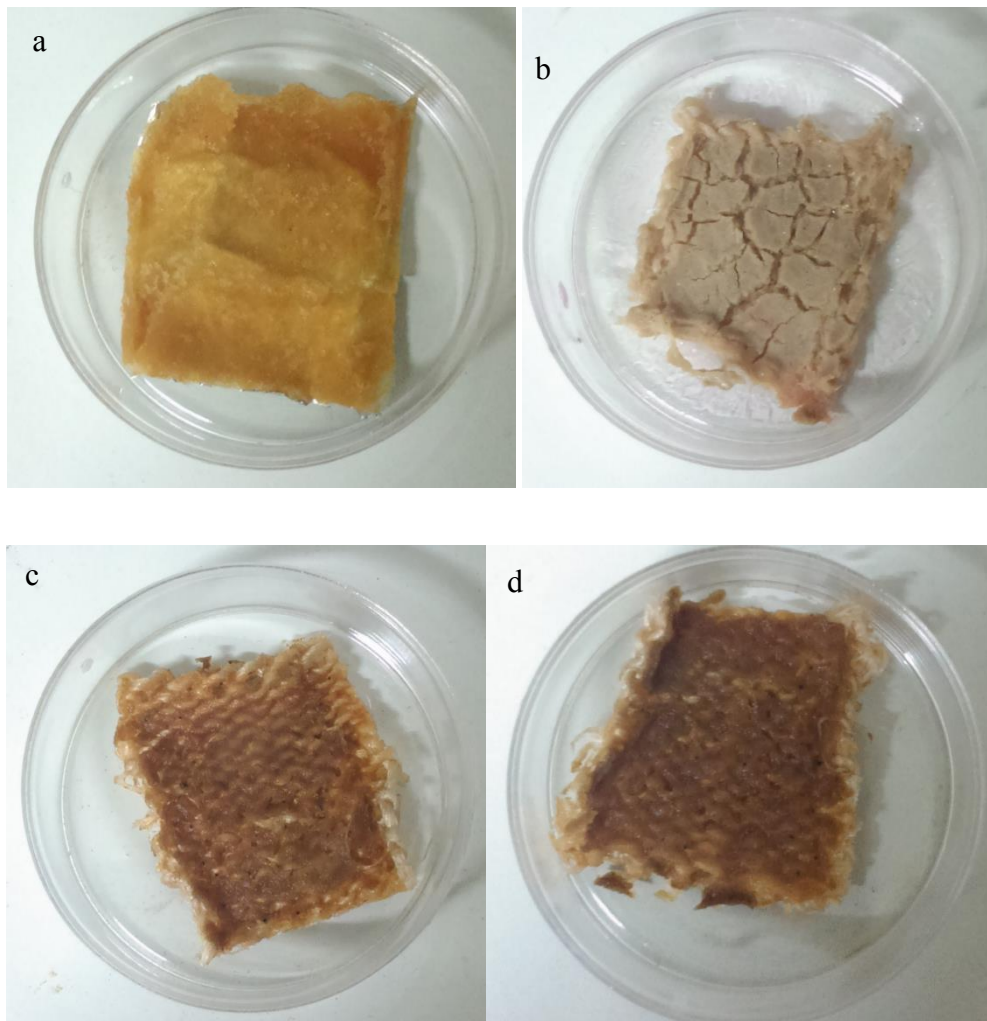


**Figure 14: Silk/Chitosan sponges overlaid on knitted silk based scaffold (a) 2% (b) 4% (c) 6% and (d) 8% silk/chitosan concentration**

### 5.1.3.1 XRD of Silk/Chitosan Sponge

The XRD peak of silk/chitosan sponge showed aberrant disturbances in peaks indicating that the sponge mainly constituted of amorphous deposits with low crystallinity. A broad peak was observed around  $22^\circ$  is indicative of chitosan particles and that of  $30^\circ$  indicates presence of silk (Figure 15).

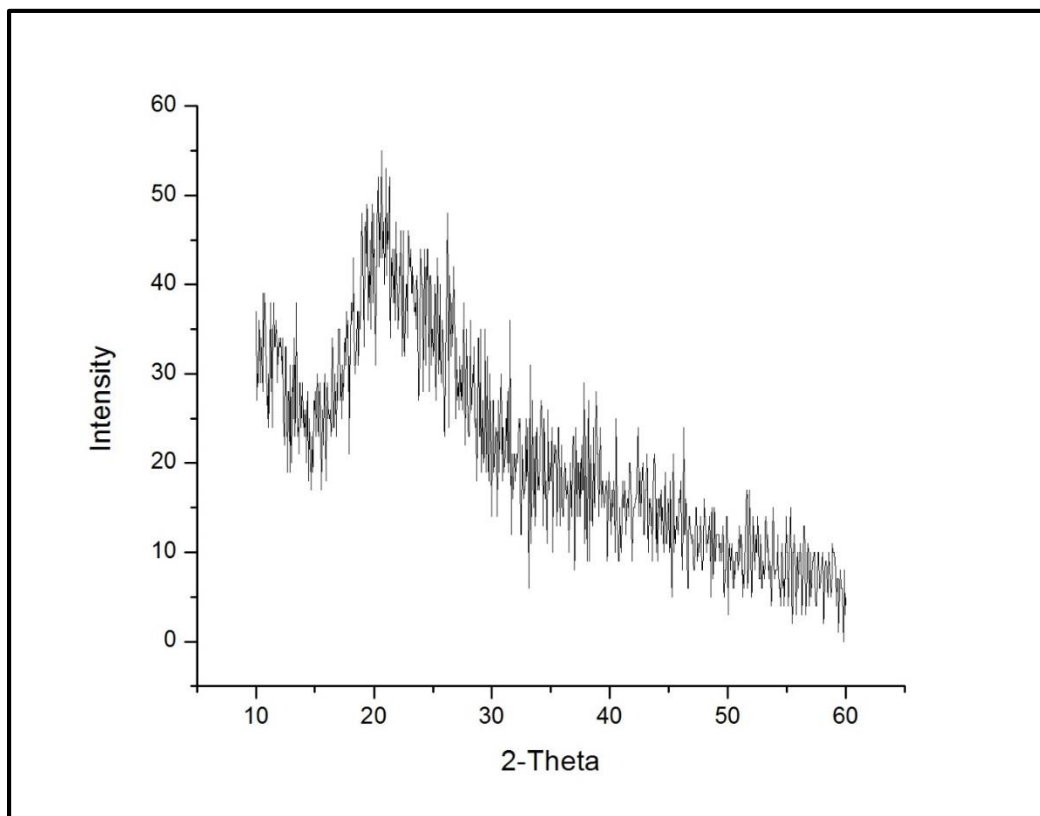
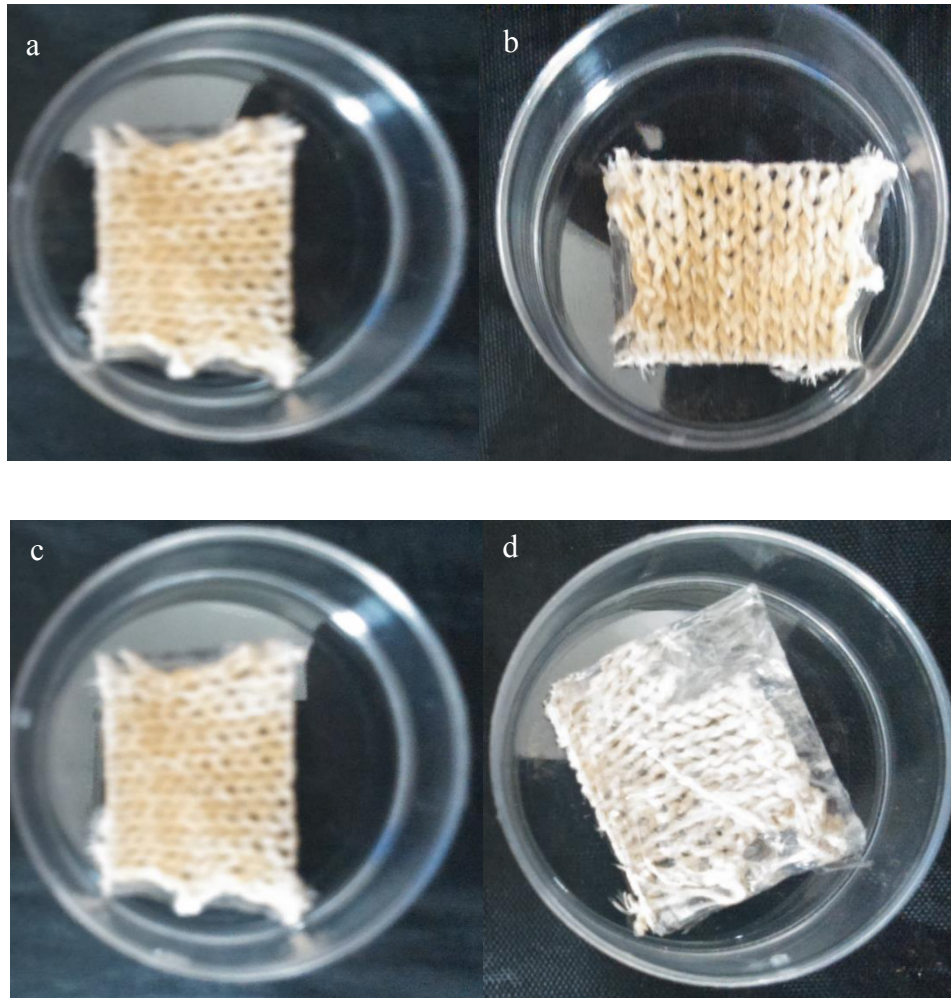


Figure 15: XRD of Silk/Chitosan sponge overlaid on knitted silk based scaffold

### 5.1.4 Morphology of Polyvinyl Alcohol Coated Knitted Silk

Polyvinyl alcohol is a clear polymer which is dissolved in distilled water and layered over knitted silk scaffold by simple drying. The polymer layer appeared as a clear coating over the knitted silk mesh. Increasing the concentration of PVA made the scaffold thicker and harder, though no change was observed visually in the transparency of the layering. PVA coating was observed to be favourable for the interaction with body fluids because the

absorption of water by the scaffold was rapid. It was also observed that as the scaffold tended to curl on itself as it absorbed more water.



**Figure 16: PVA coated knitted silk based scaffold (a) 4% (b) 6% (c) 8% (d) 12%**

#### **5.1.4.1 XRD of Polyvinyl Alcohol Coating over Knitted Silk**

Since pure PVA powder was used for the synthesis of the coating over the knitted silk scaffold, the XRD peak was expected to show a single peak in addition to the knitted silk peak. The strong narrow peak around  $19.4^\circ$  shows the presence of PVA and the high crystallinity of the coating (Figure 17).



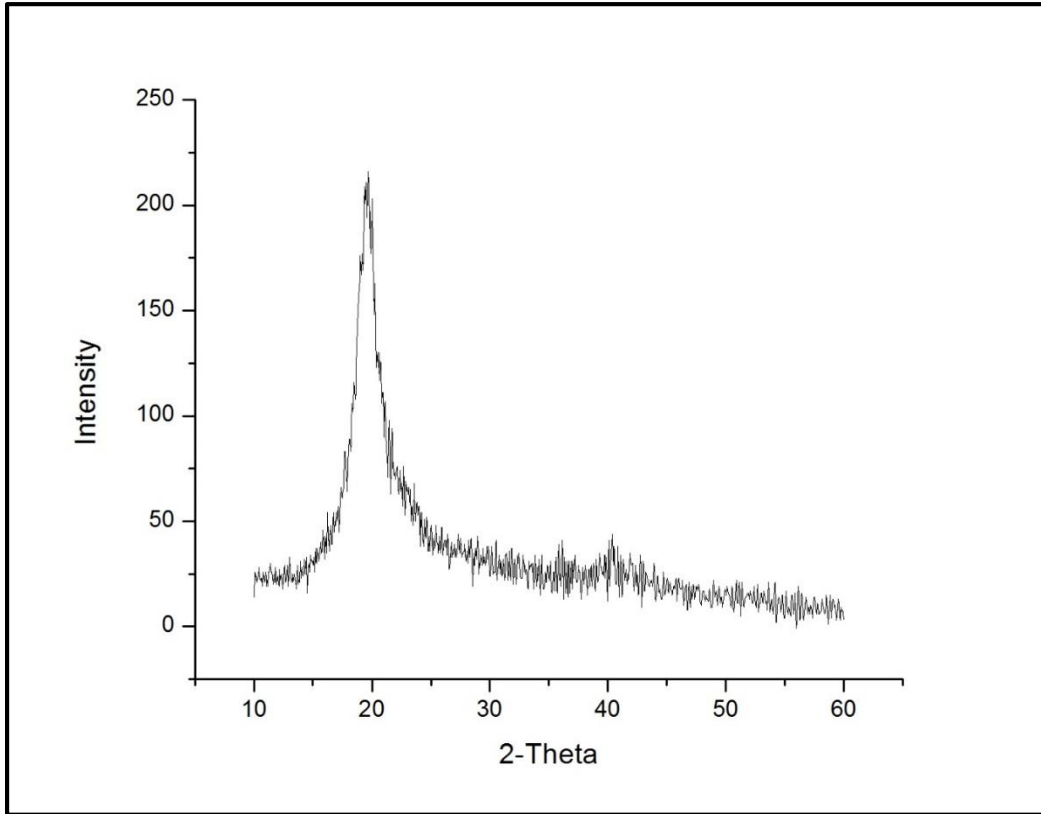


**Figure 17: XRD analysis of PVA coated knitted silk based scaffold**

## **5.2 MECHANICAL STRENGTH TESTING**

The ultimate tensile strength of the knitted silk scaffold was carried out by observing the breaking load of the scaffold. Since the knitted silk forms the base and mechanical support structure for the entire scaffold, the testing of this structure alone was assumed as sufficient to provide an average idea of the strength of the final scaffold with the application of polymer coating. The mechanical strength testing was carried out as an exercise to determine the average degradation rate of the scaffold in body fluids. For this purpose, the knitted silk fibres were immersed in PBS solution prepared at pH 7 and incubated in CO<sub>2</sub> incubator at 37°C. After the stipulated time which was assigned to each scaffold, they were subjected to tensile strength testing.

It was observed that as a thumb of rule, the longer the scaffold was immersed in PBS, the weaker its structure became. The breaking force of the dry scaffold at day 0 (before being

immersed in the buffer solution) was found to be  $44 \pm 0.2$  MPa. The decrease in strength of the scaffold with time was almost linear. At 7<sup>th</sup> day, the ultimate breaking force of the knitted silk fibres were observed to be  $39 \pm 0.61$  MPa. At the end of 30 days, the strength of the scaffold had decreased to an average of  $29.5 \pm 0.53$  MPa. This study shows that the scaffold lost its strength almost 33% over a period of 30 days. The strength of the material was found to increase marginally with the addition of polymer materials such as Hydroxyapatite, PVA and Silk/Chitosan blend (Figure 18).

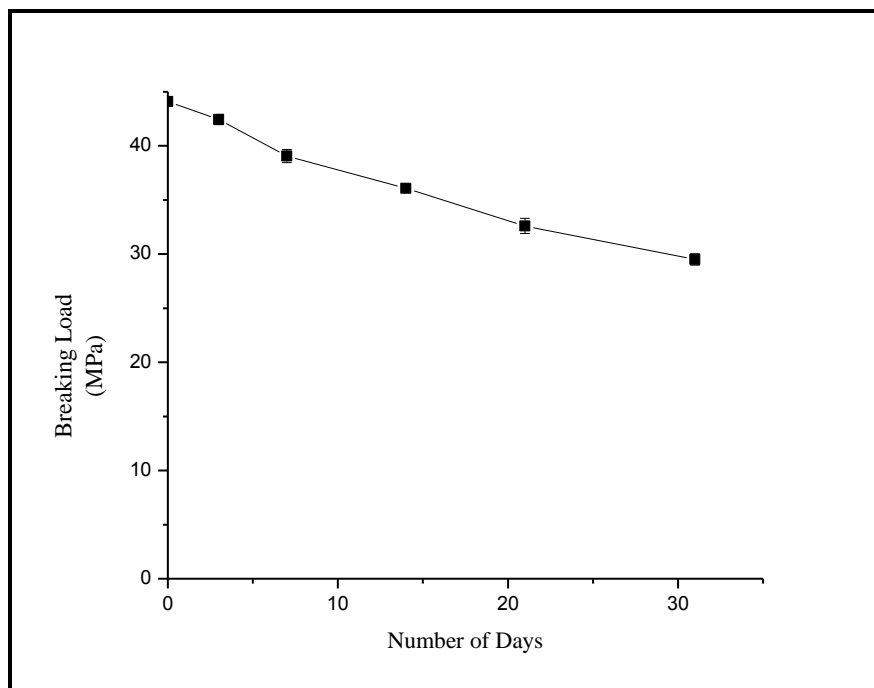


**Figure 18: Mechanical strength testing of knitted silk based scaffold immersed in PBS over a period of time to analyze the degradation of the scaffold.**

### 5.3 WATER ABSORPTION STUDIES

**5.4** The study was carried out to learn the water absorption capability and capacity of the knitted silk scaffold layered with different polymer coatings. The scaffolds were immersed in PBS solution at 37°C and observed for changed in weight for an interval of 60 minutes until there was so concurrent change in scaffold wet weight observed. The difference

between the final and initial weights of the scaffold gave an interpretation of the water absorption capacity of the scaffold.

#### 5.4.1 Water Absorption Study for Hydroxyapatite

The hydroxyapatite coated portion of the knitted silk scaffold was found to possess least capability for water absorption. Over a period of 360 minutes, the hydroxyapatite-knitted silk scaffold was able to absorb a total of 74.5% of its weight of PBS, which was attained by the scaffold coated with 10 cycles of alternate soaking process for hydroxyapatite. Even with increasing water absorption in the beginning, the values suddenly declined as the number of alternate soaking process increased. It was also observed that all the scaffolds equally absorbed water within a duration of 200 minutes after which there was minimal change in absorption. Owing to its maximum absorption capacity, this variant of alternate soaking process was used to carry out further studies over the scaffold (Figure 19,20).

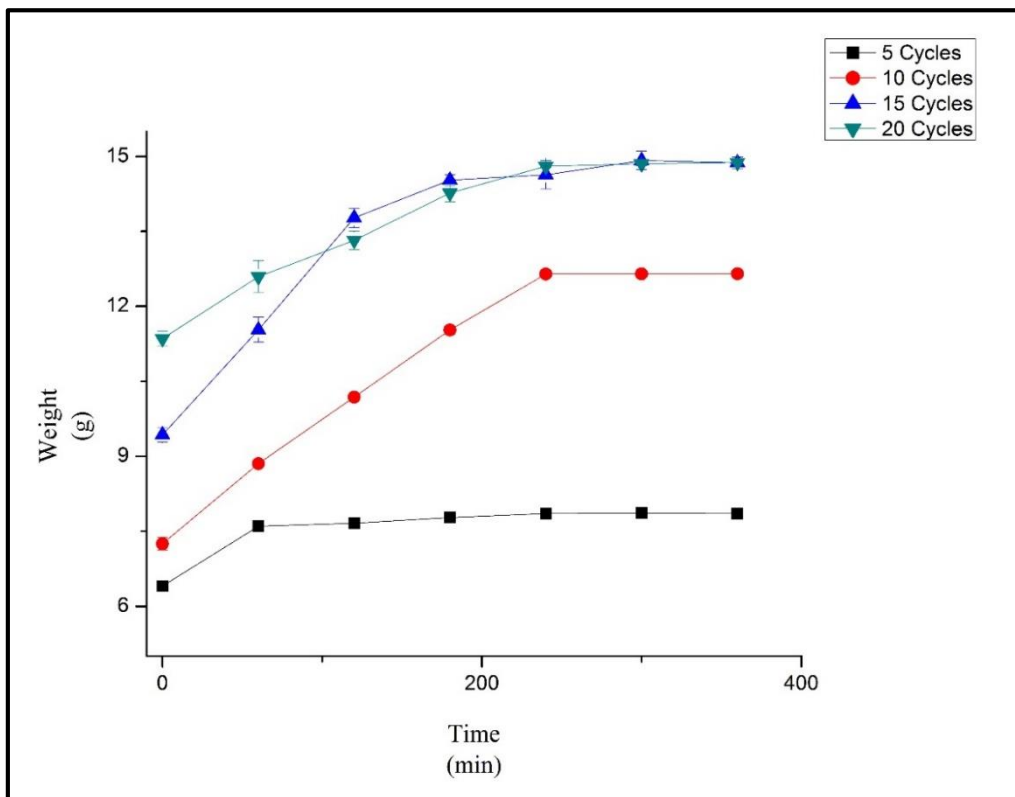


**Figure 19: Water absorption study of Hydroxyapatite coated knitted silk scaffold**

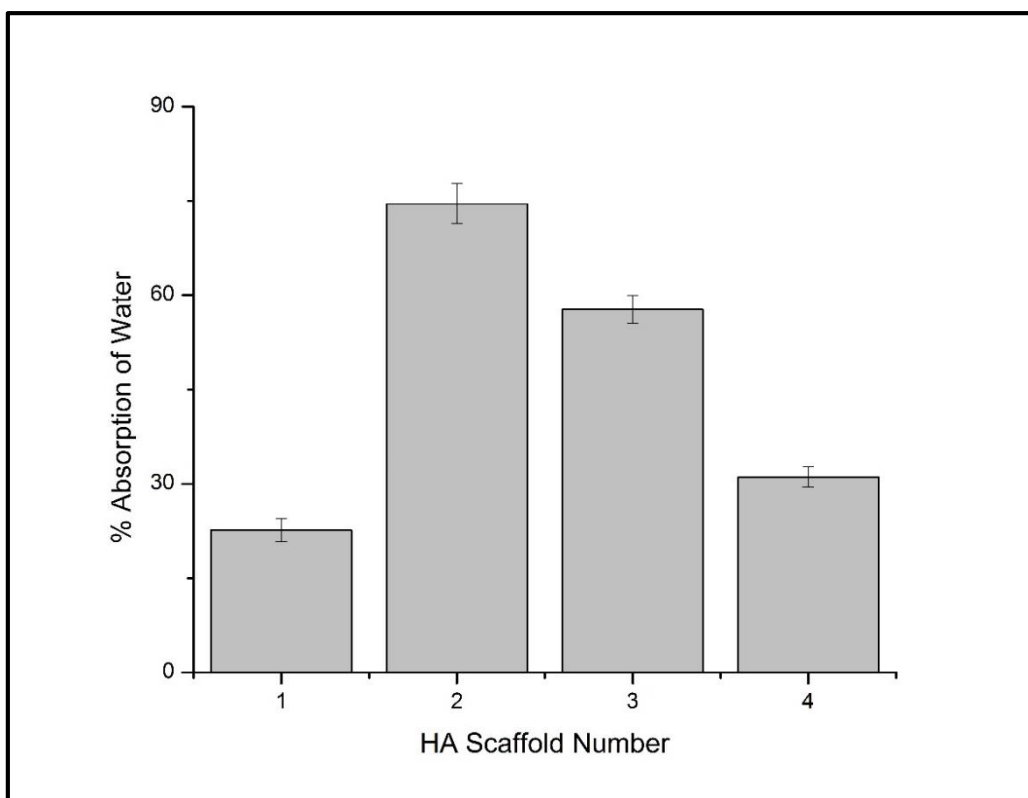


**Figure 20: Percentage of water absorption by hydroxyapatite scaffold**

#### **5.4.2 Water Absorption Study for Silk/Chitosan**

The water absorption capability of silk/chitosan sponge on the knitted silk scaffold was found to be intermediate between that of the hydroxyapatite and the PVA coating. The percentage of water absorbed was found to be highest for the scaffold with 2% silk/chitosan concentration, with its final weight increasing almost 400% that of its initial dry weight at the end of 300 minutes. It was observed that with the increasing concentration of silk/chitosan, the sponge also tended to turn brittle when immersed in water and started dislodging itself from the knitted silk mesh. The uptake of water by the sponges was uniform and linear with the increase in concentration of silk/chitosan. The saturation point of the water absorption was reached at around 250 minutes further to which there was no significant absorption of water observed. Based on this study it was concluded that 2% silk/chitosan sponges was the ideal candidate for the final scaffold (Figure 21, 22).

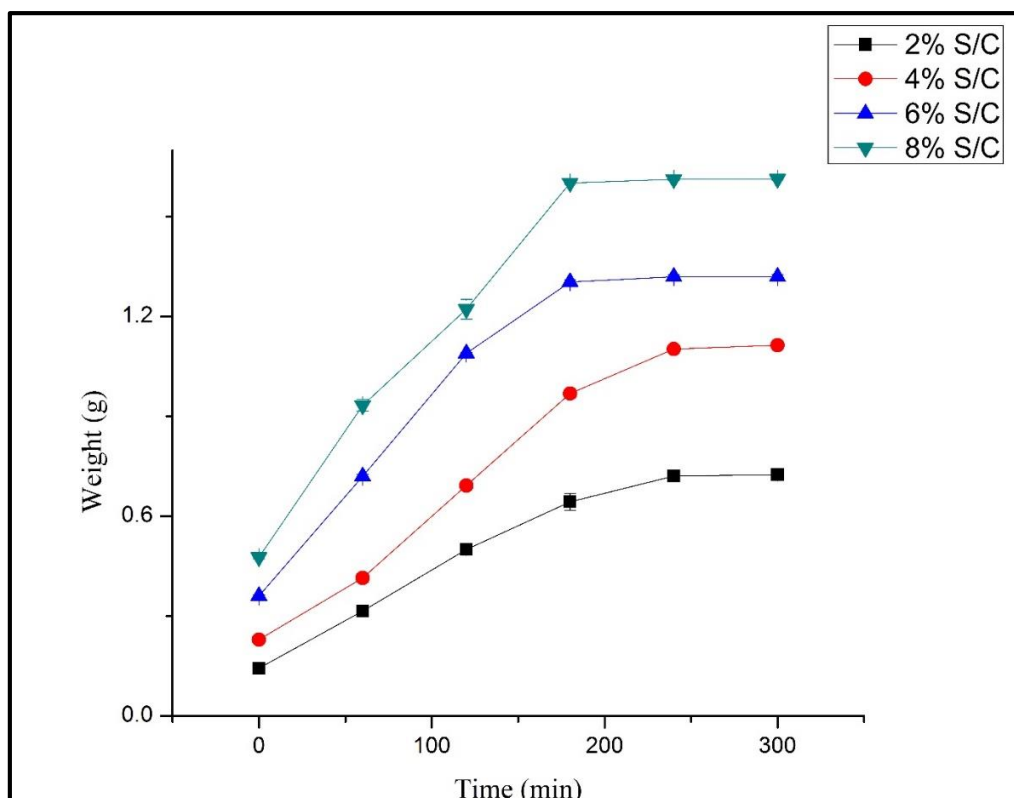


Figure 21: Water absorption study of silk/chitosan overlaid knitted silk based scaffold

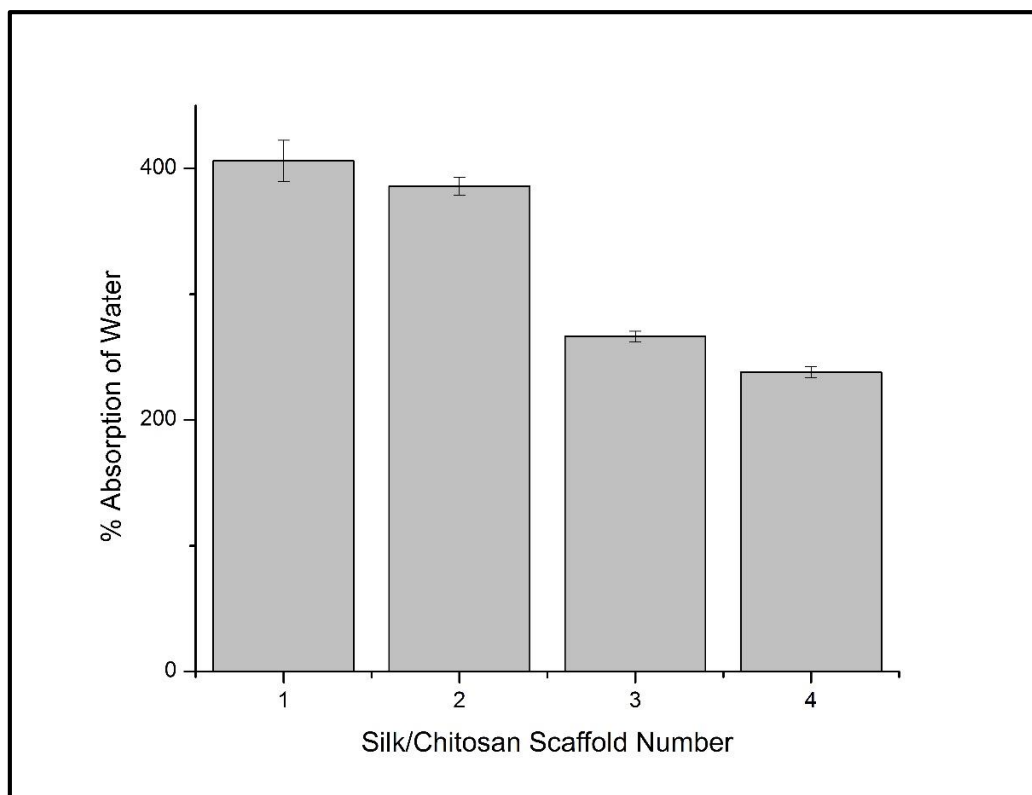
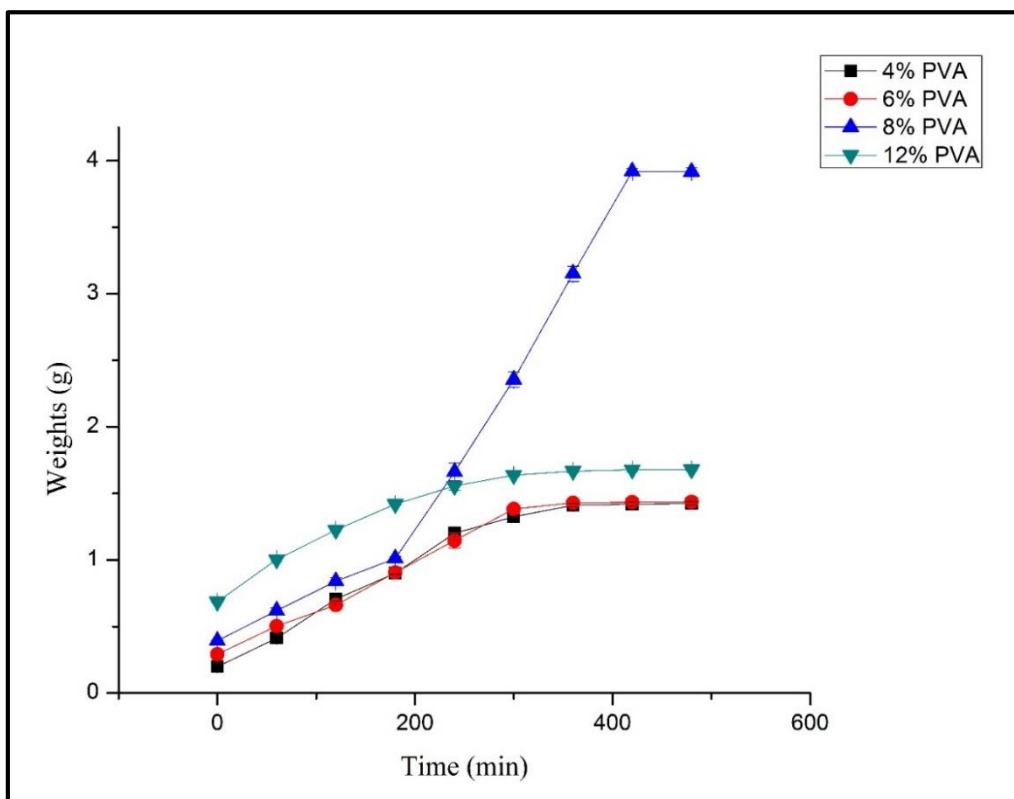


Figure 22: Percentage of water absorption by silk/chitosan overlaid knitted silk based scaffold

### 5.4.3 Water Absorption Study for Polyvinyl Alcohol

The absorption of water was found to be at the highest rate in this category of polymer coating as compared hydroxyapatite and silk/chitosan. With close to 900% increase in weight, it was clearly concluded that PVA was an ideal polymer for best results in water interaction among the three. Among the four concentrations of PVA coated on the knitted silk scaffold, the absorption capability was not found to be correlative to each other. 8% PVA coating showed the maximum water absorption capacity. The scaffolds were also observed to curl within upon interaction with PBS over the time. Scaffolds of all concentrations of PVA, except that of 8%, were found to have saturated water absorption by 300 minutes of immersion time. Owing to its outstanding water absorption capability, PVA coating of 8% (w/v) was concluded to be the ideal concentration for the final scaffold fabrication (Figure 23, 24).



**Figure 23: Water absorption study of PVA coated knitted silk based scaffold**

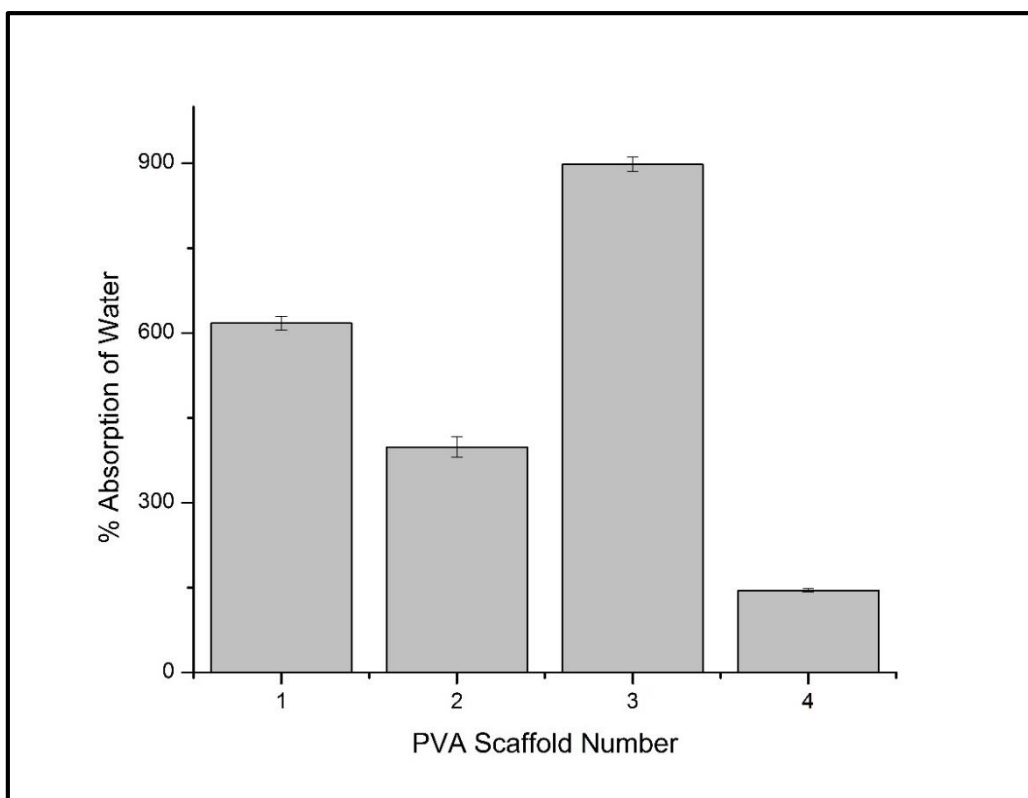


**Figure 24: Percentage of water absorption by PVA coated knitted silk based scaffold**

## **5.5 BIOCOMPATIBILITY STUDIES**

### **5.5.1 Cell Adhesion Study**

Cell adhesion study was carried out by measuring the number of cells that remain in the growth media unattached to the surface of the scaffold after 24hrs. Briefly, MG-63 osteoblasts were seeded on the hydroxyapatite coated scaffold while Saos-2 fibroblasts were seeded on silk/chitosan and PVA coated scaffolds to measure the efficiency of adhesion of cells. With an initial seeding density of  $2.8 \times 10^6$  cells/ml (MG-63) and  $2.3 \times 10^6$  cells/ml (Saos-2), the study was carried out for 24 hours subsequent to which the scaffolds were removed from the media and the unattached cells remaining in the media and those adhered to the petri dish were counted. The cell adhesion capacity was found to be  $93.3 \pm 0.42$  % efficient for MG-63 on hydroxyapatite coated scaffold;  $92.4 \pm 0.96$  % efficient for Saos-2 cells seeded on silk/chitosan scaffold; and  $94.17 \pm 0.32$  % efficient for

Saos-2 cells seeded on PVA scaffold. The high efficiency of osteoblast adherence to hydroxyapatite coated scaffold was in accordance to the previously established osteoconductive properties of the mineral. Similar correlation was drawn on the attachment efficiency of fibroblasts on silk/chitosan and PVA coated scaffold.

#### **5.5.2 Cell Proliferation Study**

MTT assay was carried out to study the proliferation rate of the cells on scaffolds. The assay gave a conclusive indication of the scaffold to be an efficient niche for cell growth and proliferations. Briefly,  $1.2 \times 10^5$  cells/ml (MG-63) was seeded on hydroxyapatite coated scaffold while a concentration of  $1.6 \times 10^5$  cells/ml (Saos-2) was seeded on both silk/chitosan scaffold and PVA coated scaffold. At the end of 3 days, the cell density was found to be  $2.6 \times 10^5$  cells/ml for MG-63 on hydroxyapatite coated scaffold,  $3.1 \times 10^5$  cells/ml for Saos-2 on silk/chitosan scaffold and  $3.3 \times 10^5$  cells/ml for Saos-2 cells on PVA coated scaffold. At the end of 7 days, the number of osteoblasts on the hydroxyapatite scaffold increased to  $9.1 \times 10^5$  cells/ml (Figure 25) while the number of fibroblast cells on silk/chitosan and PVA coated scaffolds had increased to  $9.4 \times 10^5$  cells/ml and  $9.5 \times 10^5$  cells/ml respectively (Figure 26). The assay concluded that alternate soaking process for the coating of hydroxyapatite on knitted silk scaffold was a favourable method for osteoconduction. It also confirmed that for similar kind of cells and equal seeding density, PVA was much biocompatible than silk/chitosan coating in terms of cell growth potential. Overall, it was also proved that all the three coatings performed on knitted silk scaffold were successful in providing the microenvironmental conditions for cell growth and proliferation.



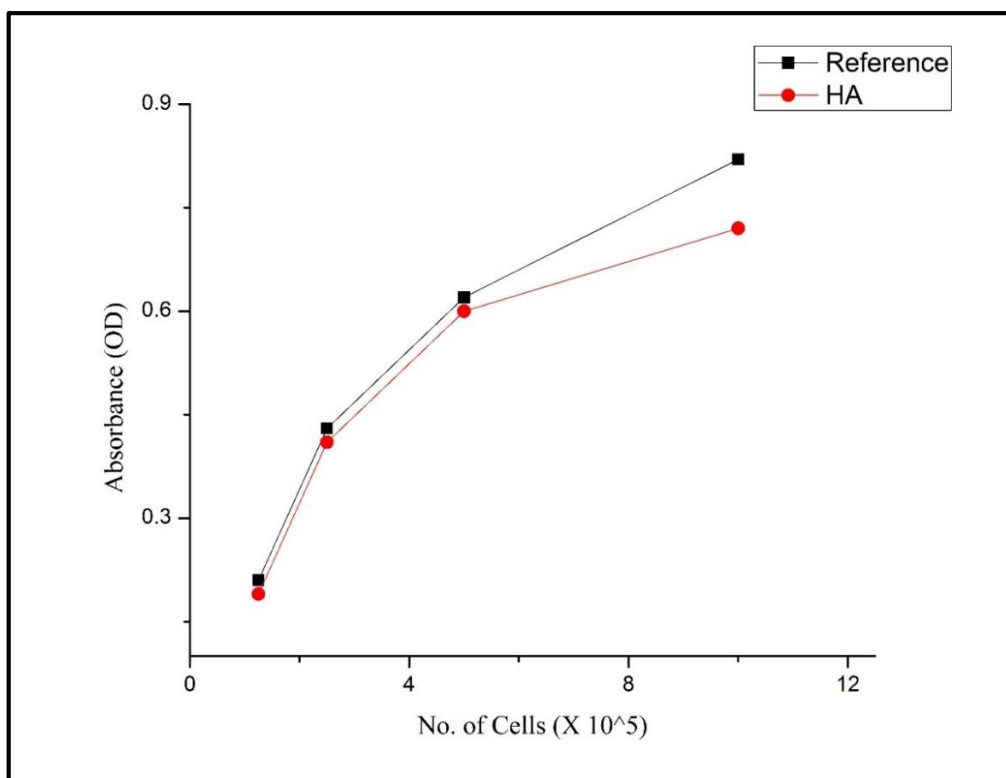


**Figure 25: MTT assay to study proliferation of MG-63 on HA coated knitted silk based scaffold**

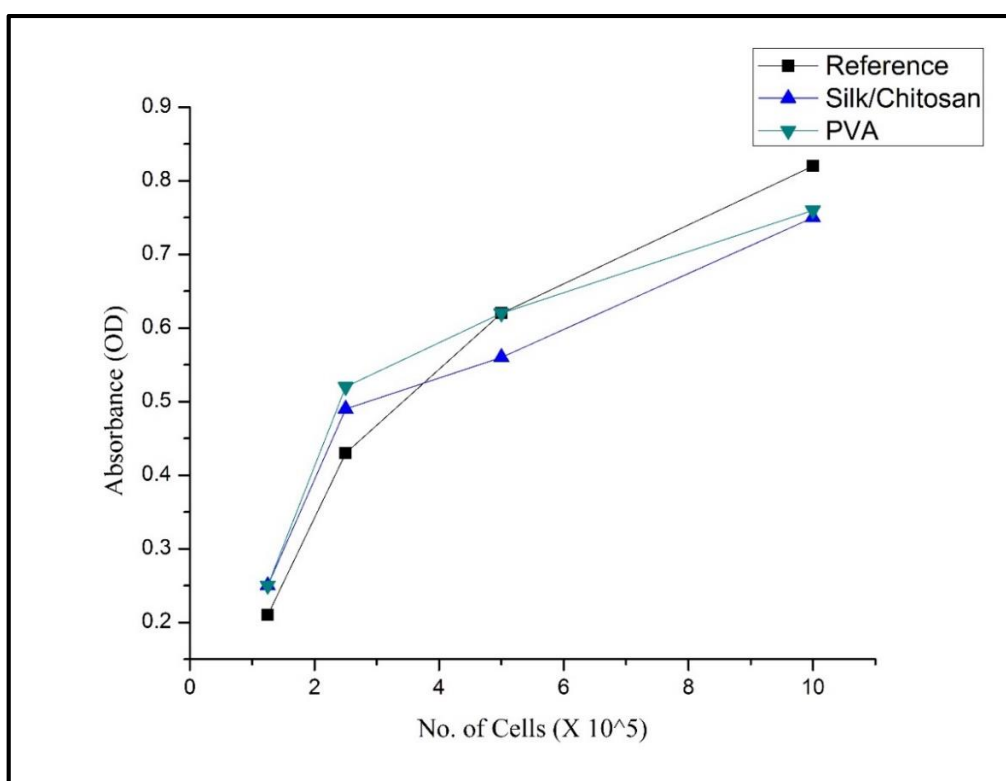


**Figure 26: MTT assay to study proliferation of Saos-2 on silk/chitosan and PVA coated knitted silk based scaffold**

## 5.6 PROPERTIES OF HYBRID SCAFFOLD

The water absorption capability was tested for the hybrid scaffold with compartmentalized coatings of all 3 polymers – hydroxyapatite, silk/chitosan and polyvinyl alcohol. The study showed that the hybrid scaffold absorbed satisfactory amounts of water and increased its final weight by almost 251% of its initial weight (Figure 27).

Cell adhesion study was carried out by seeding  $2.5 \times 10^6$  cells/ml of Saos-2 equally over all the layers of the scaffold and incubated at 37°C in CO<sub>2</sub> incubator for 24 hours. Upon removal of scaffold and examination for the remnant cells in the solution, it was found that the media showed a cell density of  $1.6 \times 10^5$  cells/ml indicating cell adhesion efficiency of the scaffold to up to 93.4% (Figure 28).

Cell proliferation assay (MTT) was carried with an initial seed of Saos-2 cells  $2.5 \times 10^5$  cells/ml. Over a period of 3 days the number of cells had increased to  $4 \times 10^5$  cells/ml and by the end of the experimental period of 7 days the cell count had increased to  $1.01 \times 10^6$  cells/ml. The result showed that the hybrid scaffold coated with different polymers was ideally favourable for the growth and proliferation of cells and could be used further for the construction of 3D hybrid scaffold for the fabrication of bone-(entheses)-ligament-(entheses)-bone tissue graft for replacing injured ligaments.

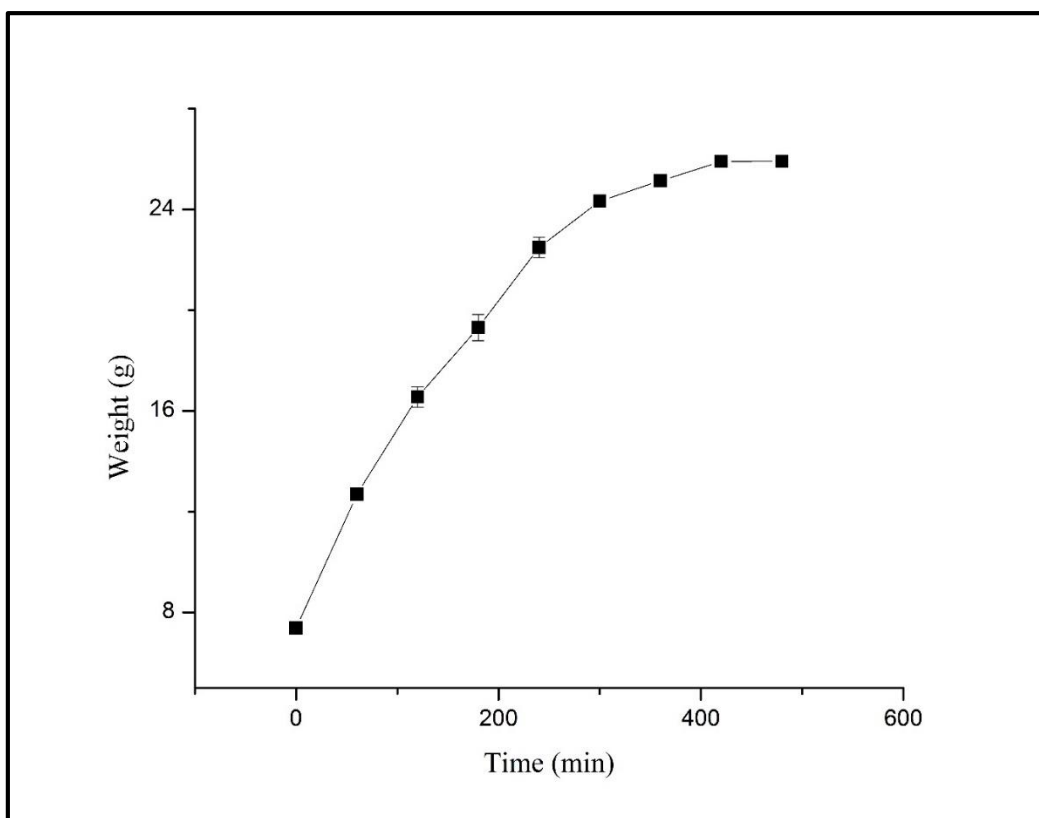


**Figure 27: Water absorption study of hybrid knitted silk based scaffold**

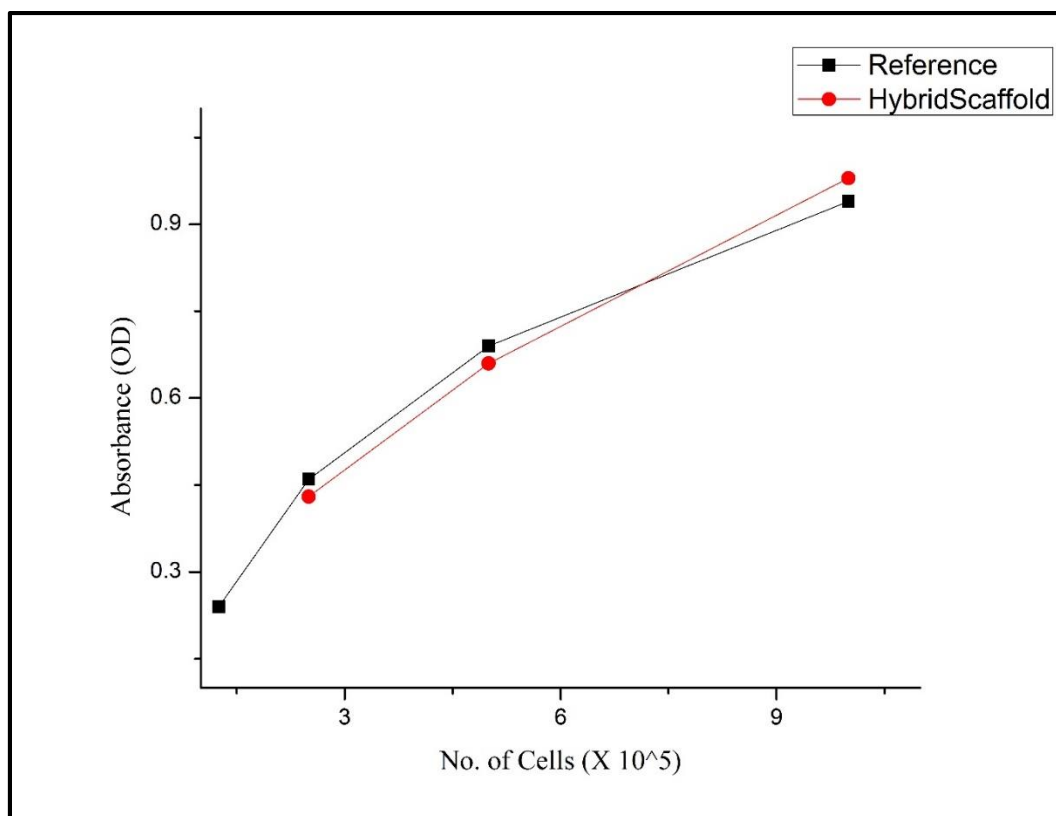


**Figure 28: MTT assay to study the proliferation of Saos-2 on hybrid knitted silk scaffold**

# **CHAPTER – 6**

# **CONCLUSION**

The anterior cruciate ligament is one of the most crucial ligaments of the body with one of the highest cases of injury related maladies of the organ. Out of the several methods that are available, tissue engineering is the best sought out method for the rectification of the injury. However, the tissue engineering experiments are not usually successful because of the failure of the ligament to integrate to the bone and form a firm bond, due to which the result is that the organ either usually fails to grow, or integrate and hence slips off, or both. Due to these problems there has been a large number of study to rectify this problem. The current study had focused on fabrication of a knitted silk based scaffold for the growth of not only ligament but also the associated tissues such as fibrocartilaginous enthesis and bone so that the integration of the bone to the ligament is an easy process. The scaffold that was fabricated was a multi-compartmental knitted silk mesh on which coatings of biopolymers were applied. For the efficient growth of cells, hydroxyapatite was coated to help growth of osteoblasts, silk/chitosan sponge was overlaid for the growth of enthesis tissue and PVA was incorporated for the growth of ligament cells or stem cells which will differentiate into ligament cells. Various methods were employed in the coating of these polymers such as alternate soaking technique, freeze drying and plain coating. A number of studies such as biocompatibility, water absorption, mechanical strength and morphological characterization were carried out on the coatings to prove them as good candidates for the growth and proliferation of cells. The results showed that the coatings had good water absorption, good mechanical strength provided by the knitted silk mesh and satisfactorily biocompatible to validate the scaffold as a good source to implant bone-ligament-bone tissue grafts.

# **CHAPTER – 7**

## **REFERENCES**

## REFERENCES

1. Bucknall TE, Teare L, Ellis H. The choice of a suture to close abdominal incisions. *Eur Surg Res* 1983;15:59–66.
2. Pennisi E. Tending tender tendons. *Science* 2002;295:1011.
3. Beynnon BD, Fleming BC. Anterior cruciate ligament strain invivo: a review of previous work. *J Biomech* 1998;31:519– 25.
4. Vunjak-Novakovic G, Altman G, Horan R, Kaplan DL. Tissue engineering of ligaments. *Annu Rev Biomed Eng* 2004;6:131–56.
5. Noyes FR, Grood ES. The strength of the anterior cruciate ligament in humans and Rhesus monkeys. *J Bone Jt Surg Am* 1976;58:1074–82.
6. C. T. Laurencin and J. W. Freeman, “Ligament tissue engineering: an evolutionary materials science approach,” *Biomaterials*, vol. 26, no. 36, pp. 7530–7536, 2005.
7. Albright JC, Carpenter JE, Graf BK, Richmond JC. Knee and leg: soft-tissue trauma. Orthopaedic knowledge, update 6. American Academy of Orthopedic Surgery; 1999.
8. H. Fan, H. Liu, S. L. Toh, and J. C. H. Goh, “Anterior cruciate ligament regeneration using mesenchymal stem cells and silk scaffold in large animal model,” *Biomaterials*, vol. 30, no. 28, pp. 4967–4977, 2009.
9. R. Mascarenhas and P. B. MacDonald, “Anterior cruciate ligament reconstruction: a look at prosthetics—past, present and possible future,” *McGill Journal of Medicine*, vol. 11, no. 1, pp. 29–37, 2008.
10. Z. Ge, J. C. H. Goh, and E. H. Lee, “Selection of cell source for ligament tissue engineering,” *Cell Transplantation*, vol. 14, no. 8, pp. 573–583, 2005.
11. J. W. Freeman and A. L. Kwansa, “Recent advancements in ligament tissue engineering: the use of various techniques and materials for ACL repair,” *Recent Patents on Biomedical Engineering*, vol. 1, pp. 18–23, 2008.
12. N. Scutt, C. G. Rolf, and A. Scutt, “Tissue specific characteristics of cells isolated from human and rat tendons and ligaments,” *Journal of Orthopaedic Surgery and Research*, vol. 3, no. 1, article 32, 2008.
13. H. Dunn MG, Bellincampi LD, Tria AJ, Zawadsky JP. Preliminary development of a collagen-PLA composite for ACL reconstruction. *J Appl Polym Sci* 1997;63:1423–8.

14. Lam KH, Nijenhuis AJ, Bartels H, Postema AR, Jonkman MF, Pennings AJ, Nieuwenhuis P. Reinforced poly(l-lactic acid) fibers as suture material. *J Appl Biomater* 1995;6:191–7.
15. Soong HK, Kenyon KR. Adverse reactions to virgin silk sutures in cataract surgery. *Ophthalmology* 1984;91:479–83.
16. Rossitch Jr. E , Bullard DE, Oakes WJ. Delayed foreign-body reaction to silk sutures in pediatric neurosurgical patients. *Childs Nerv Syst* 1987;3:375–8.
17. T. Brune, A. Borel, T. W. Gilbert, J. P. Franceschi, S. F. Badylak, and P. Sommer, “In vitro comparison of human fibroblasts from intact and ruptured ACL for use in tissue engineering,” *European Cells and Materials*, vol. 14, pp. 78–90, 2007.
18. Liu, H. Fan, S. L. Toh, and J. C. H. Goh, “A comparison of rabbit mesenchymal stem cells and anterior cruciate ligament fibroblasts responses on combined silk scaffolds,” *Biomaterials*, vol. 29, no. 10, pp. 1443–1453, 2008.
19. A. Arthur, A. Zannettino, and S. Gronthos, “The therapeutic applications of multipotential mesenchymal/stromal stem cells in skeletal tissue repair,” *Journal of Cellular Physiology*, vol. 218, no. 2, pp. 237–245, 2009.
20. R. Mafi, S. Hindocha, P. Mafi, M. Griffin, and W. S. Khan, “Sources of adult mesenchymal stem cells applicable for musculoskeletal applications—a systematic review of the literature,” *The Open Orthopaedics Journal*, vol. 5, supplement 2-M2, pp. 242–248, 2011.
21. H. H. Lu, J. A. Cooper Jr., S. Manuel et al., “Anterior cruciate ligament regeneration using braided biodegradable scaffolds: in vitro optimization studies,” *Biomaterials*, vol. 26, no. 23, pp. 4805–4816, 2005. .
22. Liljensten E, Gisselgalt K, Edberg B, Bertilsson H, Flodin P, Nilsson A, Lindahl A, Peterson L. Studies of polyurethane urea bands for ACL reconstruction. *J Mater Sci Mater Med* 2002; 13:351–9.
23. Huss, F.R.(2005):In vitro and in vivo studies of tissue engineering in reconstructive plastic surgery, Linköping.
24. Matyas, J.R..(1994): Analyzing nuclear shape as a function of relative spatial position in the femoral insertion of the medial collateral ligament. *Computer Methods and Programs in Biomedicine* 44, 69- 77.



24. Benjamin M, Kumai T, Milz S, Boszczyk AA and Ralphs JR. The skeletal attachments of tendons-tendon 'entheses' *comp biochem physiol A Mol Integr Physiol*, 2002;133:931-945.
25. Woo, S.L.Y., Buckwalter and J.A.: Injury and Repair of the Musculoskeletal Soft Tissues. American Academy of Orthopaedic Surgeons, Park Ridge, Illinois, 1988.
26. Amiel, D., Frank, C., Harwood, F., Fronek, J. and Akeson, W., (1984): Tendons and ligaments: a morphological and biochemical comparison. *Journal of Orthopaedic Research*, 1, 257- 265.
27. Kastelic, J., Palley, I., and Baer, E., (1978): The multicomposite ultrastructure of tendon, *Connective Tissue Research*, 6, 11- 23.
28. Matyas, J.R., Anton, M.G., Shrive, N.G., and Frank, C.B., (1995): Stress governs tissue phenotype at the femoral insertion of the rabbit MCL. *Journal of Biomechanics*, 28, 147- 157.
29. Sadler TW, Langman's Medical Embryology. 6th ed, JN Gardner. (1990), Baltimore: Williams & Wilkins. 411.
30. Reilly, G. C. and Currey, J. D. (1999): The development of microcracking and failure in bone depends on the loading mode to which it is adapted. *J. Exp. Biol.* 202, 543–552.
31. Stock UA, V.J.: Tissue engineering: current state and prospects. *Annu Rev Med.*, (2001). 52, 443-51.
32. Athanasiou KA, N.G., and Agrawal CM.: Sterilization, toxicity, biocompatibility and clinical applications of polylactic acid/polyglycolic acid copolymers. *Biomaterials.*, 1996.